

**CONFINED COUNTERIONS SURROUNDING A MACROION - A FIELD  
THEORETIC APPROACH**

By

Leandro Boonzaaier



Dissertation presented for the degree of Doctor of Philosophy at Stellenbosch University

Promoter : Prof. Kristian K. Müller-Nedebock

Co-promoter : Prof. Frederik G. Scholtz

December 2011

## DECLARATION

By submitting this dissertation electronically, I declare that the entirety of the work contained therein is my own, original work, that I am the sole author thereof (unless to the extent explicitly otherwise stated), that reproduction and publication thereof by Stellenbosch University will not infringe any third party rights and that I have not previously in its entirety or in part submitted it for obtaining any qualification.

Copyright © 2011 Stellenbosch University

All rights reserved

## ABSTRACT

Several experiments [1, 2, 3, 4] have shown that effective attractive interactions exist between confined like-charged macromolecules. Theoretical approaches have not reached consensus as to precisely what the mechanism for the attraction is, but it is agreed that comprehending the role of the counterion arrangement around macromolecules is crucial for understanding the effective macromolecule interactions. It is generally assumed that attraction only occurs in the limit of strong electrostatic coupling and is driven by correlation effects that are negligible in a mean-field approach, which is valid in the weak-coupling limit. However, in some experimental situations attraction occurs even in the limit of weak-coupling. We consider a field-theoretic approach that includes fluctuations to study the Coulomb interactions of confined counterions with a single flexible charged spherical macromolecule that can expand or collapse uniformly by changing its radius. We show how the linearised field-theory (valid in the weak-coupling limit) is mapped onto the square-well potential of Quantum Mechanics. The confinement leads to bound states being present in the spectrum at all times. Bound states are non-perturbative and we investigate the role they play in the physics of the system. Some of the effects are rather counter-intuitive. Firstly, upon expanding the macromolecule in a fixed confinement volume, the fluctuation part of the free energy favours a decrease in the free energy. Secondly, upon increasing the temperature to high but finite values, the fluctuation contribution does not dominate the free energy as would be expected. The mathematical origins of these effects are discussed in detail and as part of the analysis we introduce a novel regularisation scheme for computing the functional determinant arising in the model considered where the cut-off is specified unambiguously in terms of physical parameters.

## OPSOMMING

Verskeie eksperimente [1, 2, 3, 4] toon dat makro-ione met gelyksoortige ladings, in 'n eindige volume, 'n effektiewe aantrekkende krag ondervind. Alhoewel daar nog geen konsensus oor die presiese meganisme vir die aantrekking bereik is nie, is dit duidelik dat die rol van “counter-ion” rangskikking rondom die makro-ione belangrik is om die effektiewe wisselwerkings te verstaan. Dit word algemeen aanvaar dat die aantrekkende krag slegs in die limiet van sterk elektrostatiese koppeling plaasvind en dat dit 'n gevolg van “counter-ion” korrelasies is wat weglaatbaar is in 'n gemiddelde veld benadering, wat geldig is in die limiet van swak elektrostatiese koppeling. Daar bestaan egter eksperimentele situasies waar die aantrekking in die limiet van swak elektrostatiese koppeling waargeneem word. Ons bestudeer die Coulomb wisselwerking tussen “counter-ions” en 'n enkele rekbare sferiese makro-ioon vanuit 'n veld-teoretiese beskouing wat fluktuasies in ag neem. Die sferiese makro-ioon kan vergroot of verklein deur sy radius uniform te verander. Ons toon aan dat die gelineariseerde veldteorie (geldig in die limiet van swak elektrostatiese koppeling) op die eindige-diepte put Kwantummeganiese model afgebeeld kan word. Die eindige volume van die sisteem het tot gevolg dat daar altyd gebonde toestande in die spektrum voorkom. Gebonde toestande is 'n suiwer nie-steuringsteoretiese effek en ons ondersoek die rol wat dit speel in die fisika van die sisteem. Die teenwoordigheid van die gebonde toestande in die spektrum het 'n paar teen-intuitiewe effekte tot gevolg. Eerstens word die vrye energie verlaag soos die makro-ioon in 'n eindige volume vergroot. Tweedens oorheers die fluktuasie bydrae nie die vrye energie met toenemende temperatuur soos verwag sou word nie. Ons bespreek die wiskundige oorsprong van hierdie effekte. As deel van die analise ontwikkel ons 'n nuwe regulariseringstegniek vir die berekening van funksionaalintegrale waar die regulariseringsparameter ondubbelsinnig in terme van fisiese hoeveelhede uitgedruk kan word.

## CONTENTS

ACKNOWLEDGEMENTS . . . . .	iv
LIST OF FIGURES . . . . .	vii
1. Introduction and Overview . . . . .	1
1.1 Typical physical features of charged classical systems . . . . .	2
1.2 Brief overview of techniques to study charged classical systems . . . . .	3
1.3 Brief overview of field-theoretical approaches to charged classical systems . . . . .	5
1.4 The coupling constant . . . . .	6
1.5 The role of curvature . . . . .	9
1.6 Motivation for the current work . . . . .	10
1.7 Brief summary of results . . . . .	12
2. The Field-Theoretic Formulation . . . . .	14
2.1 General Field-Theoretical Formulation . . . . .	14
2.2 Single Spherical Macro-ion in a Finite Volume . . . . .	16
3. Free energy: mean-field contribution . . . . .	21
3.1 Green's Function . . . . .	21
3.2 Classical Solution . . . . .	24
3.3 Mean-field contribution to the free energy . . . . .	25
4. Free energy: fluctuations . . . . .	27
4.1 Zeta-function technique . . . . .	27
4.2 Fluctuation contribution to free energy . . . . .	30
4.2.1 Numerical verification of the 1-dimensional determinants . . . . .	34
4.2.2 Regularisation . . . . .	36
5. Results and Conclusions . . . . .	40
5.1 Free energy . . . . .	40
5.2 Role of the volume exclusion . . . . .	41
5.3 High temperature behaviour . . . . .	42
5.4 Uniqueness of the regularisation prescription . . . . .	43
5.5 What have we learnt? . . . . .	44
5.6 Caveats . . . . .	45
5.7 Outlook . . . . .	45

A. The zero-mode subtracted action . . . . .	47
B. Calculation of the Green's function for the $\ell = 0$ channel . . . . .	49
C. The Partition Function for the case of added salt . . . . .	53
BIBLIOGRAPHY . . . . .	55

**LIST OF FIGURES**

4.1 Plot of the comparison of the numerical and analytical results for the fluctuation contribution for the  $l=0$  channel for  $\frac{\ell_B}{R} = \frac{1}{10}$ . The solid line represents the analytical result and the dots the data points of the numerical calculation. 35

4.2 Plot of the comparison of the numerical and analytical results for the fluctuation contribution for the  $l=0$  channel for  $\frac{\ell_B}{R} = \frac{1}{50}$ . The solid line represents the analytical result and the dots the data points of the numerical calculation. 35

4.3 Plot of the comparison of the numerical and analytical results for the fluctuation contribution for the  $l=1$  channel for  $\frac{\ell_B}{R} = \frac{1}{50}$ . The solid line represents the analytical result and the dots the data points of the numerical calculation. 36

5.1 Electrostatic energy contribution to the free energy for various values of  $\ell_B/R$ . The dashed curve represent  $\ell_B/R = 1/50$ , the solid line  $\ell_B/R = 1/100$  and dot-dashed curve  $\ell_B/R = 1/500$ , respectively. . . . . 40

5.2 Fluctuation contribution to the free energy for various values of  $\ell_B/R$ . The dashed curve represent  $\ell_B/R = 1/50$ , the solid line  $\ell_B/R = 1/100$  and dot-dashed curve  $\ell_B/R = 1/500$ , respectively. . . . . 40

5.3 The fluctuation contribution for the ordinary Debye-Hückel theory as a function of the inverse screening length. . . . . 42

5.4 Temperature dependence of the well depth. The figure shows  $(\kappa a)^2$  plotted as a function of  $\chi = \ell_B/R$ . Note that  $\ell_B$  is proportional to  $1/T$ . . . . . 43

## Acknowledgements

This dissertation is the product of many hours (years) of labour. I am certainly not the only one who laboured through it. There are many people who have both actively and passively contributed to it.

My supervisors, Kristian Müller-Nedebock and Frederik Scholtz, have both been very supportive and have provided me with guidance throughout this project. Thank you for your patience with my silly ideas and many mistakes along the way. I have really learnt a lot from working with both of you.

Kristian, thank you for further mentoring me in so many ways and providing me with opportunities to participate in activities that can only be beneficial to me on the road ahead.

All the members of the ITP and Physics Department at Stellenbosch have in some way been instrumental to my understanding of Physics and I thank them. I also acknowledge the financial support of Stellenbosch University and the National Research Foundation of South Africa.

Along the way I often had occasion to ask myself, “Am I losing my mind?”. Thanks to Hannes Kriel for providing “sanity checks” regarding physics, mathematics, South African politics and a whole host of other things at regular intervals.

It is always good to have friends who can relate to your particular circumstances. Otini Kroukamp, though on another continent, and busy with his own PhD, was always willing to listen, talk, and encourage. Thank you for a friendship that spans over many years and for all the wisdom shared with me in that time.

Tuesday evenings have come to be associated with “meeting the boys”. Thank you to Keith Whiting, Brink Kroukamp, Dieter von Fintel and Anko de Wet who have all, over many years, contributed to me being me by listening, questioning, advising, scolding and encouraging during our Tuesday evening gatherings.

All work and no play would have seen me burnt out long ago were it not for my parents-in-law, Wolfgang and Ulrike Kassier, who have over the years contributed generously to make regular holidays possible. Thank you also for your encouragement and support in so many areas that made it possible for me to focus on getting the job done.

Teaching full-time, studying part-time, and having a family at times looked to be a juggling act that simply wasn't do-able. I thank my parents for showing me that it can



be done and for imparting to me a healthy work ethic. Thank you also for all the help with Jan over the past two years. It has made life easier.

If Tuesday evenings and holidays didn't provide enough healthy distractions, then my two year old son, Jan, certainly did. Life has just never been the same again since you have arrived, but I wouldn't want it any other way.

Without Carmen, who has accompanied me on this journey from the beginning, it would certainly have been a much more difficult road. Thank you for always believing in me and my abilities, even when I didn't anymore, and for always allowing me the space to be myself. No words can properly thank you.

In many ways this PhD was a "faith crisis". At various stages I lost faith in my own abilities, faith in the system and was ready to give up. All that has passed now, and I want to express my gratitude to God in the words of Psalm 27 v 13: "I would have lost heart, unless I had believed that I would see the goodness of the Lord in the land of the living."

## LIST OF SYMBOLS

Symbol	Definition
$z_c$	Counterion valence
$\ell_B$	Bjerrum length
$\mu$	Gouy-Chapman length
$\xi$	Manning parameter
$\phi(\vec{x})$	Fluctuating field
$\phi_{SP}$	Saddle-point solution
$\eta(\vec{x})$	Fluctuations around saddle-point solution
$\lambda$	Fugacity
$a$	Macro-ion radius
$a_0$	Macro-ion radius in reference system
$R$	Confining sphere radius
$k_B$	Boltzmann's constant
$T$	Temperature
$V$	Volume available to counterions
$\mu(\vec{x})$	Measure function for counterion exclusion
$\rho_c(\vec{x})$	Counterion charge density
$\rho_m(\vec{x})$	Macro-ion charge density
$\rho(\vec{x})$	Total charge density
$z_m$	Macro-ion valence
$\psi(\vec{x})$	Fluctuating field with zero mode subtracted
$\phi_{elec}$	Electrostatic potential
$\kappa$	Inverse screening length
$N_c$	Number of counterions
$\lambda_n$	Eigenvalues of general operator $\hat{A}$ in Chapter 4
$k_1$	Eigenvalue of operator $(-\nabla^2 + \kappa^2\mu)$
$\chi$	Dimensionless quantity $k_1 R$
$L$	Regularisation cut-off

## CHAPTER 1

### Introduction and Overview

The study of electrostatic interactions in soft matter has been an active area of research for many decades. In recent years the role that electrostatics plays in biological systems has come under intense scrutiny as increasingly more physicists are turning their attention to the physics of biological systems. Many of the components of living cells are highly charged macromolecules and understanding the effective interactions of such macromolecules is important for understanding biological functioning.

In addition to the biological applications, there are also some fundamental questions concerning electrostatics in solution that are not yet fully understood. There have been several experimental discoveries in the past twenty years or so that have cast doubt on our understanding of these matters [1, 2, 3, 4]. These experiments all report the observation of an attractive interaction between like-charged macromolecules. This is certainly counter-intuitive as one of the basic facts of electrostatics, as taught at school and undergraduate level, is that like-charge objects repel each other. These experimental results led to many speculations and much debate within the physics community, and although much progress has been made in recent times, there are still a number of unanswered questions.

This phenomenon of like-charged attraction also manifests itself in biological systems. DNA is a highly charged polymer (it has an elementary charge every  $0.17nm$  along its backbone) and is observed to collapse into a torus in solution containing multivalent ions<sup>1</sup>. Intuitively one expects that, because of its high charge density, the DNA molecule would be a highly disordered coil as the charges along the backbone repel each other via the Coulomb interaction. Interestingly enough this toroidal collapse only occurs in the presence of multivalent counterions, but holds for a wide range of solution conditions, quite a number of which correspond to conditions in living matter. Comprehending this attractive behaviour is therefore relevant for understanding DNA behaviour in living cells, and not merely an academic exercise.

---

<sup>1</sup>The article in *Physics Today* September 2000 by Gelbart *et al* provides a very readable account of the physics of this phenomenon in DNA.

## 1. Introduction and Overview

### 1.1 Typical physical features of charged classical systems

What is clear from the brief description of DNA above is that the role of counterions in understanding the effective interactions between macromolecules in solution is non-trivial. The presence of counterions has a few consequences for the electrostatic interactions.

The most familiar of these is the screening of the electrostatic interaction. The long-range Coulomb interaction effectively becomes an exponentially decaying interaction.

Secondly there is the notion of counterion condensation or charge renormalisation<sup>2</sup>. The counterions are attracted to the macromolecule electrostatically and thus neutralise part of its charge. This means that the macromolecules are not interacting electrostatically with their bare charge, but with some effective charge. There has been lots of debate on exactly how to determine this effective charge [5, 6, 7], since there is a competition between the reduction in the free energy due to electrostatic attraction of the counterions to the macromolecule (thereby reducing the effective macromolecule charge), and the tendency to increase the counterion entropy. Many models for counterion condensation have been studied, but no definite answer as to how to determine the renormalised charge has yet emerged [6, 7, 8, 9, 10, 11, 12, 13, 14].

The specific geometry of the physical system plays an important role in determining the degree of condensation. For planar macromolecules, it is guaranteed that the counterions will condense, since the electrostatic attraction always dominates over the entropy [15]. For cylindrical macromolecules both effects have the same mathematical functional form and it is then a question of considering the prefactors in both these terms [15]. Very simple theoretical criteria for counterion condensation exist for cylindrical macromolecules and to a large extent these have been confirmed by simulation results [9, 16]. For unconfined spherical macromolecules the counterions all decondense into the bulk since the entropic contribution to the free energy dominates over the electrostatic energy, implying that counterion confinement is important for spherical geometry. Indeed, the experiments reporting like-charged attraction [1, 2, 3] all require the macromolecules and counterions to be confined. Netz and Naji [15, 17] also showed theoretically that the strength of the attractive force for spherical macromolecules is

---

<sup>2</sup>These two terms essentially refer to the same phenomenon. In the colloidal science literature it is known as charge renormalisation, whereas in the polyelectrolyte literature it is referred to as counterion condensation or Manning condensation (after G. Manning who first introduced the concept).

## 1. Introduction and Overview

dependent on the size of the confining volume. The smaller the confining volume, the greater the attractive component, and when deconfining the system the attraction disappears completely.

From the preceding discussion it is clear that the question of how counterions arrange themselves around macromolecules, and consequently determine the effective macromolecule charge, is an important ingredient to understanding the effective macromolecule interactions.

### 1.2 Brief overview of techniques to study charged classical systems

In this dissertation we shall focus on a field-theoretic perspective, but before we do so, we briefly mention other approaches. It is not our aim here to give a comprehensive review of these methods, but we mention them here for the sake of completeness. There are excellent reviews on all of these topics that cover various aspects in quite some detail. What makes the study of these charged classical systems particularly difficult is that, due to the long-range nature of the Coulomb force, all the particles are correlated with each other. Integrating over all possible counterion and macromolecule positions when doing the statistical physics is therefore rather difficult in the usual configuration integral approach.

Traditionally the Poisson-Boltzmann (PB) theory has been employed to study charged classical systems [5, 18]. PB theory is a mean-field theory that explicitly neglects correlations between the counterions. For a very elegant presentation that explains exactly how these correlations are neglected and a concise derivation of PB theory see the paper by Deserno and Holm [19]<sup>3</sup>.

Central to the PB theory is the Poisson-Boltzmann equation. The PB equation is simply the Poisson equation, which relates the electrostatic potential to the charge density, but with the equilibrium counterion density profile having a Boltzmann weight

$$\nabla^2\psi = 4\pi\ell_B(z_c n_0 e^{-\beta z_c \psi(\vec{r})} + \rho_m(\vec{r})). \quad (1.1)$$

$\psi$  is the electrostatic potential,  $\rho_m(\vec{r})$  represents the macromolecule charge density and the first term on the right is the counterion charge density.  $\ell_B$  is the Bjerrum length (to be defined later) and  $z_c$  is the counterion valence. The PB equation above is for the case

---

<sup>3</sup>The paper by Andelman [18] also provides a very clear presentation of PB theory and gives a very basic and readable introduction to the electrostatic properties of biological membranes.

## 1. Introduction and Overview

without added salt. This equation is highly non-linear and one sees that even on the mean-field level the analysis is already quite non-trivial.

The Poisson-Boltzmann equation can be derived in a number of ways. It can be derived from a density functional approach where the free energy functional is minimised with respect to the counterion density [20] or it follows as the saddle-point approximation to a field-theoretic action [21]. Later in this chapter we shall discuss the range of validity of the PB equation in some detail.

The key question, and the one that we shall be returning to in this dissertation, is how to include the counterion correlations. This is really where the difficulty in all of these systems comes to the fore. In the density functional theory there are various ways of accounting for the correlations, e.g. the local density approximation (LDA) [5, 22] and Debye-Hückel Hole Cavity (DHHC) [23].

Another approach to charged systems, is more of a liquid theory approach [24, 25, 26], where one is interested in computing the pair distribution function. Correlations between counterions are included by means of various types of integral equations and exactly how to do this lies in deciding which closure relations to use.

All of the techniques we have mentioned thus far are mainly theoretical approaches. There is also a significant contribution to the literature that is devoted to the simulation of such systems [27, 28, 29, 30, 31, 32, 16]. These simulations include studying the counterion density profiles at single charged macromolecules and the related issue of counterion condensation, as well as studies of the like-charged attraction problem. Simulations are particularly useful in cases where the theoretical tools are not able to give definitive answers (see later when we discuss the field-theoretic approach).

It should of course be emphasised that each of the abovementioned approaches, as well as the field-theoretic formulation has its advantages and disadvantages. The use of a particular method is often dictated by the complexity of the specific problem being studied, and the questions one is trying to answer.

One aspect that we have not explicitly mentioned here is the size asymmetry between the macromolecules and the smaller counterions. The techniques for dealing with this are discussed in quite some detail in all of the reviews that we reference above, and we emphasize again that our primary aim here was simply to show that other methods exist and that they are in fact complementary to the approach we are following in this dissertation.

## 1. Introduction and Overview

### 1.3 Brief overview of field-theoretical approaches to charged classical systems

As already mentioned, what makes the study of these charged classical systems particularly difficult is that all the particles are correlated with each other. There are several advantages to going over to a field-theoretic approach. The field theory representation reduces the manifestly many-body problem to the study of a single fluctuating field that is proportional to the electrostatic potential due to all the charged particles. Moreover, many of the techniques of Quantum Field Theory then become available for studying such classical interacting systems. For example, it can be shown that the mean-field theory (PB theory) emerges as the saddle-point approximation to the field theory [21, 33] and thermal fluctuations can be incorporated systematically by expanding around the saddle-point solution. This is exactly the loop-expansion in Quantum Field Theory.

Netz and Orland [21] introduced a general systematic field-theoretical formulation for studying charged classical systems. This was certainly not the first such work, but the most general formulation up to that point. Podgornik [33] had introduced a field theory previously, but it was specifically limited to macromolecules with a planar geometry and indeed, most of the detailed field-theoretical calculations for classical charged systems have been restricted to planar and cylindrical geometries [33, 34]. These include work on charge condensation onto planar macromolecules [35] using a two-fluid model, showing that the condensation is driven by the fluctuations of the counterions. The same authors [36] also calculated the effective interaction between two charged planar macromolecules (also using the two-fluid model), showing that there is an attractive component to the effective interaction between the macromolecules that is due to the counterion fluctuations.

The work on rod-like polyelectrolytes also makes use of the two-fluid ideas and again find that the fluctuations drive the attractive interactions [37, 38, 39]. Kardar and Golestanian [40] also considered a field-theoretic formulation of the like-charged attraction problem and classified it as one of many “fluctuation-induced” forces. One of the reasons for concentrating mainly on the planar and cylindrical geometries is that the non-linear Poisson-Boltzmann equation (see eq.(1.1)) can be solved exactly in these geometries. The spherical geometry is more problematic since an analytic solution to the non-linear Poisson-Boltzmann equation does not exist in this geometry.

## 1. Introduction and Overview

One of the problems with the field theoretical formulation, already discussed by Netz and Orland [21], is to systematically take into account the size asymmetry between the macromolecules and the counterions, and the related problem of the exclusion of the smaller counterions from the volume occupied by the macromolecules. In [10] it was noted that this leads to a screening length that is spatially varying, which presents a calculational challenge.

### 1.4 The coupling constant

In order to study these field theories systematically, Netz and co-workers introduced a dimensionless coupling constant  $\Xi$  [41, 42] that serves as a measure for determining whether the system is strongly or weakly coupled. We briefly discuss the definition of the coupling constant and the important length scales in classical charged systems. The discussion is based on [15]. For simplicity, we start the discussion with the planar geometry and will show later in the chapter that similar definitions can be made for cylindrical and spherical geometries. The first relevant length scale is obtained by comparing the thermal energy,  $k_B T$ , with the Coulomb interaction energy of the counterions  $V(r) = \frac{z_c^2 e^2}{4\pi\epsilon\epsilon_0 r}$ . The ratio is given by

$$\frac{V(r)}{k_B T} = \frac{z_c^2 \ell_B}{r}, \quad (1.2)$$

where

$$\ell_B = \frac{e^2}{4\pi\epsilon\epsilon_0 k_B T} \quad (1.3)$$

is the Bjerrum-length. It is the distance at which two elementary charges have their Coulomb interaction energy equal to the thermal energy. A convenient quantity is the rescaled Bjerrum length, defined as

$$\tilde{\ell}_B = z_c^2 \ell_B. \quad (1.4)$$

The remaining length scales are set by the specific geometry under consideration. For the planar case consider a charged wall with a surface charge density  $\sigma_s$ . The Coulomb interaction energy between the charged wall and a counterion is

$$U(x) = \frac{z_c \sigma_s e^2 x}{2\epsilon\epsilon_0}, \quad (1.5)$$



with  $x$  the vertical distance from the wall. Once again considering the ratio of the Coulomb interaction energy and the thermal energy, we have

$$\frac{U}{k_{\text{B}}T} = \frac{x}{\mu}, \quad (1.6)$$

where

$$\mu = \frac{1}{2\pi z_c \ell_{\text{B}} \sigma_s} \quad (1.7)$$

is the Gouy-Chapman length and is the distance at which the interaction energy of a single counterion with the wall is equal to the thermal energy. The Gouy-Chapman length is also a measure of the thickness of the counterion layer at the charged wall [15, 17]. In principle, one can tune the system parameters such that the rescaled Bjerrum length and the Gouy-Chapman length can take on arbitrary values. It makes sense to only consider the dimensionless ratio of these two length scales

$$\Xi = \frac{\tilde{\ell}_{\text{B}}}{\mu} = 2\pi z_c^3 \ell_{\text{B}}^2 \sigma_s, \quad (1.8)$$

which is called electrostatic coupling parameter.

In the weak-coupling limit, where  $\Xi < 1$ , the mean-field theory is expected to give an accurate description of the charged system<sup>4</sup>. In this limit it is convenient to rewrite the grand-canonical partition function as

$$Z = \int [\mathcal{D}\phi] \exp \left[ \frac{\mathcal{H}[\phi]}{\Xi} \right], \quad (1.9)$$

where the Hamiltonian is typically of the form<sup>5</sup>

$$\mathcal{H}[\phi] = \frac{1}{8\pi\ell_{\text{B}}} \int d\vec{r} \phi(\vec{r}) (-\nabla^2) \phi(\vec{r}) - i \int d\vec{r} \phi(\vec{r}) \sigma(\vec{r}) - \lambda \int d\vec{r} \mu(\vec{r}) e^{-\nu\phi(\vec{r})}. \quad (1.10)$$

In the Hamiltonian above  $\sigma(\vec{r})$  represents the macromolecule charge density,  $\mu(\vec{r})$  takes the restriction on the possible counterion positions into account and  $\lambda$  is the fugacity. In the limit where  $\Xi \rightarrow 0$ , the functional integral is dominated by the value of the integrand at its saddle-point. The standard procedure in the saddle-point approximation is to expand the argument of the exponential around the saddle-point solution. The field  $\phi$  is

<sup>4</sup>We simply give a brief description of the results here. The interested reader can consult the original articles where the details are discussed quite extensively.

<sup>5</sup>In Chapter 3 we present a detailed discussion of how to rewrite the usual configuration integral representation of the partition function in the field theoretic format.

1. Introduction and Overview

written as

$\phi(\vec{r}) = \phi_{SP}(\vec{r}) + \sqrt{\Xi}\eta(\vec{r})$  and the formal expansion of the Hamiltonian is

$$H[\phi] = H[\phi_{SP}] + \sum_{j=2}^{\infty} \frac{\Xi^{j/2}}{j!} \int \frac{\delta^j H[\phi]}{\delta\phi(\vec{r}_1) \dots \delta\phi(\vec{r}_j)} \Big|_{\phi=\phi_{SP}} \eta(\vec{r}_1) \dots \eta(\vec{r}_j) d\vec{r}_1 \dots d\vec{r}_j, \quad (1.11)$$

where  $\phi_{SP}$  is the saddle-point solution and is obtained from the equation

$$\frac{\delta\mathcal{H}[\phi]}{\delta\phi(\vec{r})} \Big|_{\phi=\phi_{SP}} = 0. \quad (1.12)$$

The differential equation obtained by taking the functional derivative above is the Poisson-Boltzmann equation, the solution of which, as we shall demonstrate in the next chapter, gives the average electrostatic potential. The  $\eta$ s in eq.(1.11) are the fluctuations around the saddle-point. In field theory the expansion above is known as the loop-expansion.

For  $\Xi \gg 1$  the saddle-point approximation breaks down and a simple expansion around the saddle-point solution is no longer appropriate. In [41, 42], Netz and Moreira present a method for studying field theories of charged systems in the limit of strong coupling. The grand-canonical partition function is rewritten as

$$Z = Z_0 \sum_{j=0}^{\infty} \frac{1}{j!} \left[ \frac{\Lambda}{2\pi\Xi} \right]^j \prod_{k=1}^j \int d\vec{r}_k \exp \left[ -\Xi \sum_{n < m}^j v(\vec{r}_n) - v(\vec{r}_m) - \sum_{i=1}^j u(\vec{r}_i) \right]. \quad (1.13)$$

The factor  $Z_0$  represents the system with all the counterions removed and is given by

$$Z_0 = e^{\frac{-U_0}{\pi\Xi}}, \quad (1.14)$$

and

$$U_0 = \frac{1}{8\pi} \int d\vec{r} d\vec{r}' \sigma(\vec{r}) v(\vec{r} - \vec{r}') \sigma(\vec{r}') - \frac{Q}{4\pi} \int d\vec{r}' v(\vec{r}' - \vec{r}_0) \sigma(\vec{r}'). \quad (1.15)$$

The  $\sigma$  represents charge distribution of the macroions in our earlier description and  $u(\vec{r}_i)$  represents the interaction of a single counterion with the macromolecule. The  $v(\vec{r} - \vec{r}')$  represents the two-particle interaction. The expansion of the partition function is similar to a virial expansion where  $\Lambda$  is the rescaled fugacity. The strong-coupling theory is obtained in the limit  $\Xi \rightarrow \infty$  of the expansion above.

Netz and co-workers showed that the two asymptotic limits,  $\Xi \rightarrow 0$  and  $\Xi \rightarrow \infty$  are

indeed accurately described by the mean-field theory and their strong-coupling theory respectively. In the intermediate range where the coupling constant takes on finite values there is still much debate on how to analyse such charged systems and one has to resort to other methods. It is here that simulations play an important role, since it is able to give insight into the physics in this intermediate range. Most of the experimental realisations of such charged systems lie in this intermediate range for the coupling constant.

### 1.5 The role of curvature

As already mentioned in the previous section, the geometry of the macromolecule plays a significant role in the physics of such charged systems. For cylindrical systems Manning [43] introduced the so-called Manning parameter which is defined as

$$\xi = \frac{a}{\mu}, \quad (1.16)$$

where  $a$  is the radius of curvature of the cylinder and  $\mu$  is the Gouy-Chapman length. The Manning parameter is a measure of the deviation from planar geometry [17]. For large  $\xi$ , that is  $a \gg \mu$ , one expects the behaviour to be qualitatively similar to the planar case. For cylinders there is ample evidence that for  $\xi > 1$  counterion condensation takes place, whereas for  $\xi < 1$  there is complete diffusion of counterions into the bulk. There is thus a threshold value Manning parameter  $\xi_c = 1$  for cylinders. The Gouy-Chapman length for cylinders is defined as

$$\mu = \frac{1}{2\pi z_c \ell_B \sigma_s} = \frac{a}{z_c \ell_B \tau} \quad (1.17)$$

with  $\tau = 2\pi\sigma_s a$  the linear charge density. The corresponding Manning parameter is

$$\xi = z_c \ell_B \tau, \quad (1.18)$$

and the coupling constant is then defined as

$$\Xi = \frac{z_c^3 \ell_B^2 \tau}{a}. \quad (1.19)$$

A similar concept can be introduced for spherical macromolecules [9, 15] using the same basic definition for the Gouy-Chapman length. For spheres the Gouy-Chapman length is

defined as

$$\mu = \frac{1}{2\pi z_c \ell_B \sigma_s} = \frac{2a^2}{z_c \ell_B z_m}, \quad (1.20)$$

where  $z_m = 4\pi\sigma_s a^2$  is the total charge valency of the macromolecule. The corresponding Manning parameter is

$$\xi = \frac{z_c \ell_B z_m}{2a}, \quad (1.21)$$

and the coupling constant

$$\Xi = \frac{z_c^3 \ell_B^2 z_m}{2a^2}. \quad (1.22)$$

Here  $a$  now refers to the radius of the sphere. For spheres there is no simple criterion as to what the threshold value for the Manning parameter,  $\xi_c$  is. There is evidence that suggests that it depends on the confinement volume [15, 17].

It is generally assumed that the attractive effective interaction between like-charged macromolecules is observed only in the strong-coupling limit [15, 17]. This assumption is usually motivated as follows. It is assumed that the non-trivial behaviour is driven by the counterion-correlations. For  $\Xi \ll 1$  the mean-field theory is adequate to capture the physics and in this region correlations between the counterions can be neglected. For curved macromolecules it is further assumed that together with a large value for the coupling constant, the corresponding Manning parameter has to be sufficiently large too [15, 17], making it more planar-like. However, the experiments in [1, 2, 3] reporting like-charged attraction between spherical colloidal particles, all have experimental parameters that set the coupling constant to values in the range  $\Xi \sim 10^{-2} - 10^{-1}$  [15], which places it inside the range of validity of the weak-coupling theory. It thus seems as if the situation is not as clear as one would hope.

## 1.6 Motivation for the current work

The motivation for the current work is based on the following observations. We have already mentioned some of them in previous sections, but we list them again for the sake of completeness.

- (i) Neu [44] showed analytically, and for an arbitrary geometry, that the full non-linear Poisson-Boltzmann theory is unable to account for the like-charged attraction between macromolecules. The non-linearities are therefore not solely responsible for non-trivial behaviour.

- (ii) There are experimental situations where the coupling constant is indeed in the range of the weak-coupling theory, but attractive interactions between macromolecules are observed.
- (iii) The like-charged attraction for spherical particles only occurs when the macromolecules are contained inside a finite volume, and the strength of the attraction is inversely proportional to the size of the confining volume.
- (iv) The macromolecule curvature plays a central role in the effective valence it carries, and therefore in the effective interactions between macromolecules.

In the light of these observations it is important to reconsider the counterion correlations (fluctuations), especially in the weak-coupling limit and in a finite volume. Furthermore, we explicitly study the macro-ion curvature by considering the macro-ion to be flexible, and assuming that it can expand or collapse uniformly by changing its radius. However, we do not assign any mechanical properties to this expansion or collapse and essentially assume that the macro-ion has no stiffness. One could also think of this as considering whether there is an effective interaction between the macro-ion and the confining walls of the system.

Although we are not directly considering like-charged attraction in this study, from the discussion in previous sections it is clear that understanding counterion arrangements around single macro-ions is important, since they directly influence the effective interactions.

We consider a field-theoretic approach to calculating the partition function for counterions and salt in a finite volume surrounding a single spherical macro-ion. We study a linearised theory, valid in the high temperature limit, that includes fluctuation and correlation effects. The fact that the linearised theory is valid in the high temperature limit already places it in the range of validity of the weak-coupling theory, since the coupling constant behaves like  $\Xi \sim \ell_B^2$ . In this work we show that in the linearised theory of spherically confined counterions and salt that are also excluded from the concentric macro-ion, the field theory can be mapped onto the finite square well problem in quantum mechanics. In three dimensions the usual finite square well potential in an infinite volume only has bound states forming when the potential well has a certain minimum depth [45], but in a finite volume there is always at least one bound state formed, regardless of the well depth.

The central objective of this dissertation can now be stated:

**It is a well-known fact that bound states cannot be obtained perturbatively, therefore the presence of bound states in the spectrum signal some remnant of non-perturbative effects, even in the linearised weak-coupling limit. The question we wish to answer is exactly what role the bound states play, specifically in the fluctuation contribution, and whether they have some non-trivial effect on the physics of such a charged system. Could the role of the bound states in this simplified model provide some insight into the mechanism for like-charged attraction in the weak-coupling limit?**

At this point it is worth mentioning the paper by Baumgartl *et al.* [46] that claim the like-charged attraction between colloidal particles observed experimentally in [1, 2, 3] is nothing but an artefact due to optical distortions when doing the video microscopy. As mentioned earlier, like-charged attraction also manifests itself in biological systems such as DNA condensation, so it is certainly an observable effect. Furthermore, direct numerical simulations of confined charged colloidal particles [47, 28, 29] report like-charged attraction between colloids over a wide range of coupling constant values. The strong-coupling theory also predicts like-charged attraction for a variety of geometries, including spherical particles. These theoretical and numerical considerations and the disagreement between the different experimental results highlight the fact that the situation is far from being clearly understood. It serves as further motivation for revisiting the weak-coupling limit to see if any non-trivial effects can be observed.

### 1.7 Brief summary of results

This classification of the spectrum of the finite square well potential in terms of bound states and scattering states, allows for a clearer mathematical understanding of the behaviour of the fluctuation contribution to the free energy. The bound states dominate the fluctuation contribution and lead to non-perturbative effects that would be missed if one were to treat the calculation of the fluctuation contribution perturbatively. One such effect is the decrease in the free energy upon decreasing the volume available to the counterions and salt ions. One would expect the fluctuation contribution to increase the free energy in this case, since there is apparently a loss of entropy for the smaller ions, but there are correlations between the smaller ions that make this decrease possible. These correlations are encoded in the bound state contribution to the fluctuations and

we are able to give a precise mathematical expression for this.

Another counter-intuitive effect observed is that at high, but finite, temperature the fluctuation contribution to the free energy does not dominate. One would expect that as the temperature increases the fluctuation contribution should at some point become the dominant contribution to the free energy. In this model that does not happen, and yet again one can explain that in terms of the mapping of the problem onto the finite square well potential and the formation of bound states.

Clearly these non-perturbative effects are not due to non-linearities in the field theory. They arise due to the structure of the spectrum of the operator in the linearised field theory. As is well-known, bound states cannot be obtained perturbatively and it is in this sense that we say the effect described above is non-perturbative. As we explain in Chapter 5, any attempt to model the volume exclusion of the counterions and salt ions by some effective screening length, will not observe the abovementioned non-perturbative contribution to the fluctuation part of the free energy.

Computing the fluctuation contribution to the free energy involves calculating functional determinants. For this we apply and adapt a recently developed technique by Kirsten and co-workers [48, 49, 50] for computing such functional determinants in terms of a generalised zeta-function. Furthermore, we develop a novel regularisation technique for the determinant calculation such that the cut-off is unambiguously given entirely in terms of physical parameters.

More than simply answering the central question about observing non-trivial behaviour in the linearised theory, the calculational techniques presented in this paper could serve as a starting point for more complicated calculations. The Poisson-Boltzmann equation does not have an analytical solution in spherical geometry and the linearised model considered in this dissertation could, with a few minor modifications, form the basis for variational calculations in spherical geometry. Furthermore, the insight gained in the bound states and their role in encoding non-perturbative effects, could only serve to give a variational ansatz a richer structure.

## CHAPTER 2

### The Field-Theoretic Formulation

In Chapter 1 we discussed some of the features of the field-theoretic approach to charged systems without actually showing how a field theory is constructed. We shall do so in this chapter. The technique is very straightforward and we shall keep the discussion as general as possible before moving over to the system we want to study.

#### 2.1 General Field-Theoretical Formulation

Consider a system of macro-ions interacting electrostatically with  $N_c$  counterions in solution. For simplicity we assume that there is no added salt<sup>6</sup>. The macro-ions are considered as extended objects with valence  $z_m$ , and we assume the counterions to be point-like particles with valence  $z_c$ . The electrostatic interaction energy of such a system, scaled by the thermal energy  $k_B T$  is given by

$$\begin{aligned}
 \beta H &= \frac{\ell_B}{2} \int d\vec{x}_1 \int d\vec{x}_2 \rho_m(\vec{x}_1) \frac{1}{|\vec{x}_1 - \vec{x}_2|} \rho_m(\vec{x}_2) + \frac{\ell_B}{2} \int d\vec{x}_1 \int d\vec{x}_2 \rho_c(\vec{x}_1) \frac{1}{|\vec{x}_1 - \vec{x}_2|} \rho_c(\vec{x}_2) \\
 &- \ell_B \int d\vec{x}_1 \int d\vec{x}_2 \rho_m(\vec{x}_1) \frac{1}{|\vec{x}_1 - \vec{x}_2|} \rho_c(\vec{x}_2) \\
 &= \frac{\ell_B}{2} \int d\vec{x}_1 \int d\vec{x}_2 \rho(\vec{x}_1) \frac{1}{|\vec{x}_1 - \vec{x}_2|} \rho(\vec{x}_2),
 \end{aligned} \tag{2.1}$$

where  $\rho_m(\vec{x})$  is the macro-ion charge density (still unspecified) and for point-like counterions we have  $\rho_c(\vec{x}) = z_c \sum_{i=1}^{N_c} \delta(\vec{x} - \vec{y}_i)$ .

The configuration part of the canonical partition function is

$$\begin{aligned}
 Z &= \int \prod_{i=1}^{N_c} \frac{d\vec{x}_i}{V} \mu(\vec{x}_i) e^{-\beta H} \\
 &= \int \prod_{i=1}^{N_c} \frac{d\vec{x}_i}{V} \mu(\vec{x}_i) e^{-\frac{\ell_B}{2} \int d\vec{x}_1 \int d\vec{x}_2 \rho(\vec{x}_1) \frac{1}{|\vec{x}_1 - \vec{x}_2|} \rho(\vec{x}_2)},
 \end{aligned} \tag{2.2}$$

where we are integrating over all possible counterion configurations. In eq.(2.2),  $V$  is the volume available to the counterions and  $\mu(\vec{x})$  is a measure function that accounts for the

---

<sup>6</sup>Adding salt does not change any of the qualitative features that we shall discuss, but simply leads to a redefinition of the screening length. See Appendix C for details.



exclusion of the counterions from the volume occupied by the macro-ions.

The Hamiltonian in eq.(2.1) contains the self-energies for macro-ions and counterions.

The macro-ion self-energy will be subtracted explicitly later when we compute the mean-field contribution to the free energy in Chapter 3. The counterion self-energy manifests itself in the divergence of the fluctuation contribution to the free energy (the functional determinants) to be computed in Chapter 4, and is dealt with in the regularisation scheme discussed in that chapter.

The expression for the partition function as it is written in eq.(2.2) is difficult to evaluate because all the particles are correlated with each other. Since the Hamiltonian is quadratic in  $\rho$  we can introduce the functional integral form for the partition function by performing a Hubbard-Stratonovich transformation [40]:

$$e^{-\frac{1}{2} \int d\vec{x}_1 \int d\vec{x}_2 \psi(\vec{x}_1) \hat{A}(\vec{x}_1, \vec{x}_2) \psi(\vec{x}_2)} = \frac{1}{Z_0} \int [\mathcal{D}\phi] e^{-\frac{1}{2} \int d\vec{x}_1 \int d\vec{x}_2 \phi(\vec{x}_1) \hat{A}^{-1}(\vec{x}_1, \vec{x}_2) \phi(\vec{x}_2) + i \int d\vec{x} \psi(\vec{x}) \phi(\vec{x})},$$

where  $Z_0 = (\det A^{-1})^{-1/2}$ . In the rest of this work,  $Z_0$  will not play any further role, so we simply drop it. For the specific case of the Coulomb interaction, the inverse of the operator  $V(\vec{x}_1, \vec{x}_2) = \frac{\ell_B}{|\vec{x}_1 - \vec{x}_2|}$  is [21]

$$V^{-1} = -\frac{\nabla^2 \delta(\vec{x}_1 - \vec{x}_2)}{4\pi\ell_B}. \quad (2.3)$$

Substituting, we obtain the following expression for the partition function;

$$\begin{aligned} Z &= \int [\mathcal{D}\phi] \int \prod_{i=1}^{N_c} \frac{d\vec{x}_i}{V} \mu(\vec{x}_i) e^{-\frac{1}{8\pi\ell_B} \int d\vec{x}_1 \int d\vec{x}_2 \phi(\vec{x}_1) (-\nabla^2) \delta(\vec{x}_1 - \vec{x}_2) \phi(\vec{x}_2) + i \int d\vec{x} \rho(\vec{x}) \phi(\vec{x})} \\ &= \int [\mathcal{D}\phi] \int \prod_{i=1}^{N_c} \frac{d\vec{x}_i}{V} \mu(\vec{x}_i) e^{-\frac{1}{8\pi\ell_B} \int d\vec{x} \phi(\vec{x}) (-\nabla^2) \phi(\vec{x}) + i \int d\vec{x} (\rho_m(\vec{x}) - \rho_c(\vec{x})) \phi(\vec{x})}. \end{aligned}$$

If we insert the expression for the counterion charge density into the functional integral, we have for the last term in the exponential

$$\begin{aligned} -i \int d\vec{x} \rho_c(\vec{x}) \phi(\vec{x}) &= -i \int d\vec{x} z_c \sum_{i=1}^{N_c} \delta(\vec{x} - \vec{x}_i) \phi(\vec{x}) \\ &= -i z_c \sum_{i=1}^{N_c} \phi(\vec{x}_i). \end{aligned} \quad (2.4)$$

The partition function thus becomes

$$\begin{aligned}
Z &= \int [\mathcal{D}\phi] e^{-\frac{1}{8\pi\ell_B} \int d\vec{x} \phi(\vec{x})(-\nabla^2)\phi(\vec{x}) + i \int d\vec{x} \rho_m(\vec{x})\phi(\vec{x})} \left( \frac{1}{V} \int \prod_{j=1}^{N_c} d\vec{x}_j \mu(\vec{x}_j) e^{-\sum_j^{N_c} iz_c \phi(\vec{x}_j)} \right). \\
&= \int [\mathcal{D}\phi] e^{-\frac{1}{8\pi\ell_B} \int d\vec{x} \phi(\vec{x})(-\nabla^2)\phi(\vec{x}) + i \int d\vec{x} \rho_m(\vec{x})\phi(\vec{x})} \left( \frac{1}{V} \int d\vec{x} \mu(\vec{x}) e^{-iz_c \phi(\vec{x})} \right)^{N_c} \\
&= \int [\mathcal{D}\phi] e^{-\frac{1}{8\pi\ell_B} \int d\vec{x} \phi(\vec{x})(-\nabla^2)\phi(\vec{x}) + i \int d\vec{x} \rho_m(\vec{x})\phi(\vec{x}) + N_c \ln \left( \frac{1}{V} \int d\vec{x} \mu(\vec{x}) e^{-iz_c \phi(\vec{x})} \right)}. \tag{2.5}
\end{aligned}$$

The integration over the counterion coordinates was performed explicitly and the complicated configuration integral has been replaced by a functional integral over a single field. We shall see later that this field is proportional to the electrostatic potential due to all the charged particles in the system. The difficulty of the problem is now that one is left with a very non-linear field theory.

The partition function as it appears in eq.(2.5) is exact for arbitrary macro-ion geometry and charge distribution as we have not yet specified  $\rho_m$  and  $\mu(\vec{x})$ . The only assumption thus far is that the counterions are point-like particles.

## 2.2 Single Spherical Macro-ion in a Finite Volume

We now consider a single spherical macro-ion with radius  $a$  at the centre of a larger concentric sphere with radius  $R$ . For this system, the measure function  $\mu(\vec{x})$  is defined as

$$\mu(\vec{x}) = \begin{cases} 0 & \text{if } |\vec{x}| < a \\ 1 & \text{if } |\vec{x}| > a, \end{cases}$$

and the macro-ion charge density is simply  $\rho_m(\vec{x}) = z_m \delta(\vec{x})$ . The spherical symmetry of the problem allows us to make this simplifying assumption about the macro-ion charge density and place the charge at the centre. This will yield the same results as a macro-ion charge density that is smeared out on the surface of the macro-ion.

As mentioned in Chapter 1, we are interested in investigating the weak-coupling limit, i.e. evaluate the functional integral using a saddle-point approximation. For the spherical geometry the last term in the action is problematic since it will give rise to the non-linear Poisson-Boltzmann (PB) equation for the saddle-point solution. It is well known that no analytic solution exists for the PB equation in spherical geometry. In order to make any progress we have to approximate this term and we do so by expanding

both the exponential and logarithm to quadratic order [21]. This approximation is valid in the high temperature or equivalently low density limits, and therefore immediately places our study in the range of validity of the weak-coupling theory of Netz and co-workers as introduced in Chapter 1. Performing the expansion we find

$$\begin{aligned} N_c \ln \left( \frac{1}{V} \int d\vec{x} \mu(\vec{x}) e^{-iz_c \phi(\vec{x})} \right) &\approx N_c \ln \left( \frac{1}{V} \int d\vec{x} \mu(\vec{x}) \left( 1 - iz_c \phi(\vec{x}) - \frac{1}{2} z_c^2 \phi^2(\vec{x}) \right) \right) \\ &= i \frac{N_c}{V} \int d\vec{x} \mu(\vec{x}) \phi(\vec{x}) - \frac{N_c}{2V} \int d\vec{x} \mu(\vec{x}) \phi^2(\vec{x}) \\ &\quad + \frac{N_c}{2} \left( \frac{1}{V} \int d\vec{x} \mu(\vec{x}) \phi(\vec{x}) \right)^2. \end{aligned}$$

The action is now

$$\begin{aligned} \mathcal{H}[\phi] &= -\frac{1}{8\pi\ell_B} \int d\vec{x} \phi(\vec{x}) (-\nabla^2) \phi(\vec{x}) - i \int d\vec{x} \rho_m(\vec{x}) \phi(\vec{x}) + i n_c \int d\vec{x} \mu(\vec{x}) \phi(\vec{x}) \\ &\quad - \frac{1}{2} n_c \int d\vec{x} \mu(\vec{x}) \phi^2(\vec{x}) + \frac{N_c}{2} \left( \frac{1}{V} \int d\vec{x} \mu(\vec{x}) \phi(\vec{x}) \right)^2, \end{aligned}$$

where  $n_c = \frac{N_c}{V}$  is the concentration of counterions in the solution. If we write  $\phi(\vec{x}) = \tilde{\phi} + \psi(\vec{x})$ , where  $\tilde{\phi} = \frac{1}{V} \int d\vec{x} \phi(\vec{x})$ , we note that the action becomes <sup>7</sup>

$$\begin{aligned} \mathcal{H}[\psi] &= -\frac{1}{8\pi\ell_B} \int d\vec{x} \psi(\vec{x}) (-\nabla^2) \psi(\vec{x}) - i \int d\vec{x} \rho_m(\vec{x}) \psi(\vec{x}) + i n_c \int d\vec{x} \mu(\vec{x}) \psi(\vec{x}) \\ &\quad - \frac{1}{2} n_c \int d\vec{x} \mu(\vec{x}) \psi^2(\vec{x}) + \frac{N_c}{2} \left( \frac{1}{V} \int d\vec{x} \mu(\vec{x}) \psi(\vec{x}) \right)^2 - \frac{1}{2} \tilde{\phi} \int d\vec{x} \nabla^2 \psi(\vec{x}). \end{aligned}$$

The last term in the action encodes the charge neutrality of the solution and can be incorporated into the boundary conditions on the fluctuating field.

If we consider

$$\begin{aligned} \int d\vec{x} \mu(\vec{x}) \phi(\vec{x}) &= \tilde{\phi} \int d\vec{x} \mu(\vec{x}) + \int d\vec{x} \mu(\vec{x}) \psi(\vec{x}) \\ &= \int d\vec{x} \mu(\vec{x}) \phi(\vec{x}) + \int d\vec{x} \mu(\vec{x}) \psi(\vec{x}), \end{aligned} \tag{2.6}$$

since  $\int \mu(\vec{x}) = V$ . Therefore,  $\int d\vec{x} \mu(\vec{x}) \psi(\vec{x}) = 0$ . If we now set  $\kappa^2 = 4\pi\ell_B n_c z_c^2$  and

<sup>7</sup>See Appendix A for details.

rearrange the terms, the partition function becomes

$$Z = \int [\mathcal{D}\psi] e^{-\frac{1}{8\pi\ell_B} \int d\vec{x} \psi(\vec{x}) [-\nabla^2 + \kappa^2 \mu(\vec{x})] \psi(\vec{x}) + i \int d\vec{x} \rho_m(\vec{x}) \psi(\vec{x})}. \quad (2.7)$$

We have used the fact that the change of variables leaves the measure of the functional integral unchanged.

Since the functional integral is Gaussian in the lowest order approximation, we can evaluate it exactly. To do this we write the field as  $\psi(\vec{x}) = \phi_{SP}(\vec{x}) + \eta(\vec{x})$  where  $\phi_{SP}(\vec{x})$  is the saddle-point solution and  $\eta(\vec{x})$  are the fluctuations around it. The saddle-point solution represents the mean-field theory [34] and  $\phi_{SP}$  satisfies the equation

$$(-\nabla^2 + \kappa^2 \mu(\vec{x}))\phi_{SP}(\vec{x}) = i4\pi\ell_B \rho_m(\vec{x}), \quad (2.8)$$

which is obtained by applying the Euler-Lagrange equations. Eq.(2.8) will be recognised as the linearised Poisson equation if we make the substitution  $\phi_{elec} = -i\phi_{SP}$ , with  $\phi_{elec}$  the electrostatic potential. Eq.(2.8) differs from the conventional Debye-Hückel theory in the important respect that the term in  $\kappa^2$  is spatially (radially) dependent. This position dependent inverse screening length is particularly difficult to deal with [10]. Note, however, that eq.(2.7) is the analog of a quantum mechanical particle in a finite square well potential, and as such facilitates dealing with this position dependent screening length. We shall see later that this mapping to the square well potential has interesting consequences for the fluctuation contribution to the free energy, in that the spectrum of the operator contains bound states which cannot be treated in a perturbative manner. The boundary conditions on  $\phi_{elec}$  are as follows:

$$\phi_-(a) = \phi_+(a) \quad (2.9)$$

$$\left. \frac{d\phi_-(r)}{dr} \right|_{r=a} = \left. \frac{d\phi_+(r)}{dr} \right|_{r=a} \quad (2.10)$$

$$\left. \frac{d\phi_+(r)}{dr} \right|_{r=R} = 0. \quad (2.11)$$

We have dropped the subscript *elec* and, unless it causes confusion, we will drop it in all subsequent sections. The subscripts + and - above denote the electrostatic potential for the regions  $r > a$  and  $r < a$  respectively. Eqs.(2.9) and (2.10) encode the continuity of the electrostatic potential and the electric field at the boundary of the macro-ion, assuming no surface charge on the macro-ion, while eq.(2.11) encodes the charge

neutrality of the solution.

We can expand the action around the mean-field solution. The result is

$$\begin{aligned}
\mathcal{H}[\psi] &= \mathcal{H}[\phi_{SP} + \eta] \\
&= \mathcal{H}[\phi_{SP}] + \int d\vec{x} \eta(\vec{x}) \left( \frac{\delta \mathcal{H}}{\delta \phi} \Big|_{\phi=\phi_{SP}} \right) + \frac{1}{2} \int d\vec{x} \int d\vec{y} \eta(\vec{x}) \left( \frac{\delta^2 \mathcal{H}}{\delta \phi^2} \Big|_{\phi=\phi_{SP}} \right) \eta(\vec{y}) \\
&= \mathcal{H}[\phi_{SP}] + \frac{1}{2} \int d\vec{x} \int d\vec{y} \eta(\vec{x}) \left( \frac{\delta^2 \mathcal{H}}{\delta \phi^2} \Big|_{\phi=\phi_{SP}} \right) \eta(\vec{y}).
\end{aligned} \tag{2.12}$$

The linear term vanishes because the classical field satisfies the equation of motion. The partition function thus becomes

$$Z = e^{-\mathcal{H}[\phi_{SP}]} \int [\mathcal{D}\eta] e^{-\frac{1}{8\pi\ell_B} \int d\vec{x} \eta(\vec{x}) [-\nabla^2 + \kappa^2 \mu(\vec{x})] \eta(\vec{x})}. \tag{2.13}$$

Consider the argument of the exponential of the first factor.

$$\begin{aligned}
\mathcal{H}[\phi_{SP}] &= \frac{1}{8\pi\ell_B} \int d\vec{x} \phi_{SP}(\vec{x}) (-\nabla^2 + \kappa^2 \mu(\vec{x})) \phi_{SP}(\vec{x}) - i \int d\vec{x} \rho_m(\vec{x}) \phi_{SP}(\vec{x}) \\
&= \int d\vec{x} \phi_{SP}(\vec{x}) \left[ \frac{1}{8\pi\ell_B} (-\nabla^2 + \kappa^2 \mu(\vec{x})) \phi_{SP}(\vec{x}) - i \rho_m(\vec{x}) \right] \\
&= -\frac{i}{2} \int d\vec{x} \phi_{SP}(\vec{x}) \rho_m(\vec{x}),
\end{aligned} \tag{2.14}$$

where we obtained the last line by using eq.(2.8). We know that the solution to eq.(2.8) is given by

$$\phi_{SP}(\vec{x}) = i4\pi\ell_B \int d\vec{y} G(\vec{y}, \vec{x}) \rho_m(\vec{y}), \tag{2.15}$$

where  $G(\vec{y}, \vec{x})$  is the Green's function of the operator  $-\nabla^2 + \kappa^2 \mu(\vec{x})$ . Substituting this into eq.(2.14) we have

$$\mathcal{H}[\phi_{SP}] = \frac{4\pi\ell_B}{2} \int d\vec{x} \int d\vec{y} \rho_m(\vec{y}) G(\vec{y}, \vec{x}) \rho_m(\vec{x}). \tag{2.16}$$

Thus the final expression for the partition function becomes

$$\begin{aligned}
Z &= e^{-\frac{4\pi\ell_B}{2} \int d\vec{x} \int d\vec{y} \rho_m(\vec{x}) G(\vec{y}, \vec{x}) \rho_m(\vec{y})} \int [\mathcal{D}\eta] e^{-\frac{1}{8\pi\ell_B} \int d\vec{x} \eta(\vec{x}) [-\nabla^2 + \kappa^2 \mu(\vec{x})] \eta(\vec{x})} \\
&= e^{-\frac{4\pi\ell_B}{2} \int d\vec{x} \int d\vec{y} \rho_m(\vec{x}) G(\vec{y}, \vec{x}) \rho_m(\vec{y})} \left( \det [-\nabla^2 + \kappa^2 \mu(\vec{x})] \right)^{-\frac{1}{2}}.
\end{aligned} \tag{2.17}$$

The case of added salt gives a partition of exactly the same form except with a redefined

inverse screening length. The details of the derivation appear in Appendix C. In this chapter we have seen how to rewrite the partition function as a functional integral. In the following chapter we compute the mean-field contribution to the free energy.

## CHAPTER 3

### Free energy: mean-field contribution

In Chapter 2 we formally rewrote the partition function as a functional integral and after linearising the action, obtained the result

$$Z = e^{-\frac{4\pi\ell_B}{2} \int d\vec{x} \int d\vec{y} \rho_m(\vec{x}) G(\vec{y}, \vec{x}) \rho_m(\vec{y})} \left( \det \left[ -\nabla^2 + \kappa^2 \mu(\vec{x}) \right] \right)^{-\frac{1}{2}}. \quad (3.1)$$

The free energy is defined as  $F = -k_B T \ln Z$ . Thus,

$$F = k_B T \frac{4\pi\ell_B}{2} \int d\vec{x} \int d\vec{y} \rho_m(\vec{x}) G(\vec{y}, \vec{x}) \rho_m(\vec{y}) + \frac{1}{2} k_B T \ln \left( \det \left[ -\nabla^2 + \kappa^2 \mu(\vec{x}) \right] \right) \quad (3.2)$$

We compute the free energy of the system as a function of the macro-ion radius within a fixed confining radius and ask whether the macro-ion expands or collapses. We choose as our reference point for the free energy, a macro-ion with a fixed radius,  $a_0$ . In this chapter we will compute the first term of the free energy in eq.(3.2), i.e. the mean-field contribution, analytically.

### 3.1 Green's Function

The restricted geometry of the system implies that the Green's function for the operator  $-\nabla^2 + \kappa^2 \mu(\vec{x})$  will not be translationally invariant. In this section we construct the Green's function and then use it to construct the solution to eq.(2.8). The Green's function is the solution to the following equation;

$$\left( -\nabla^2 + \kappa^2 \mu \right) G(\vec{r}, \vec{r}') = \delta(\vec{r} - \vec{r}'). \quad (3.3)$$

Using the representation for the  $\delta$ -function in spherical coordinates and the completeness of the spherical harmonics [51], the Green's function can be written as

$$G(\vec{r}, \vec{r}') = \sum_{l=0}^{\infty} \sum_{m=-l}^l G_{lm}(\vec{r}, \vec{r}') Y_{lm}(\theta, \phi). \quad (3.4)$$

Substituting this expression into eq.(3.3) and using the properties of the spherical harmonics, we can separate the angular dependence and find

$$G_{lm} = g_l(r, r') Y_{lm}^*(\theta', \phi'), \quad (3.5)$$

where the radial part satisfies the equation

$$\frac{1}{r} \frac{d^2}{dr^2} [r g_l(r, r')] - \left[ \frac{l(l+1)}{r^2} + \kappa^2 \mu \right] g_l(r, r') = \frac{1}{r^2} \delta(r - r'), \quad (3.6)$$

subject to the boundary conditions;

$$g_{l,-}(a, r') = g_{l,+}(a, r') \quad (3.7)$$

$$\frac{dg_{l,-}(r, r')}{dr} \Big|_{r=a} = \frac{dg_{l,+}(r, r')}{dr} \Big|_{r=a} \quad (3.8)$$

$$\frac{dg_{l,+}(r, r')}{dr} \Big|_{r=R} = 0. \quad (3.9)$$

These are the same boundary conditions for the electrostatic problem that we discussed in the previous chapter. The + (−) in  $g_+$  ( $g_-$ ) denotes the Green's function for the region  $r > a$  ( $r < a$ ). The charge density is spherically symmetrical and hence only the  $l = 0$  channel contributes to the electrostatic potential. Therefore, we only construct the Green's function for the  $l = 0$  channel.

When  $r \neq r'$ , we have to solve the homogeneous equation

$$\frac{1}{r} \frac{d^2}{dr^2} [r g_l(r, r')] - \left[ \frac{l(l+1)}{r^2} + \kappa^2 \mu \right] g_l(r, r') = 0. \quad (3.10)$$

The solution to this equation for the  $l = 0$  channel is

$$g_0(r, r') = \begin{cases} \left( \frac{A(r')}{r} + B(r') \right) \theta(a - r) + \left( C(r') \frac{e^{-\kappa r}}{r} + D(r') \frac{e^{\kappa r}}{r} \right) \theta(r - a) & \text{for } r < r' \\ \left( \frac{A'(r')}{r} + B'(r') \right) \theta(a - r) + \left( C'(r') \frac{e^{-\kappa r}}{r} + D'(r') \frac{e^{\kappa r}}{r} \right) \theta(r - a) & \text{for } r > r' \end{cases}$$

The  $\theta(x)$  above is just the usual Heaviside function. To ensure that the Green's function is regular at the origin we set  $A(r') = 0$ . By applying the boundary conditions, the condition that the Green's function should be symmetric in its arguments and the fact that the derivative of  $g(r, r')$  should be proportional to the delta function at  $r = r'$  [51],



we finally obtain<sup>8</sup>

$$g_0(r, r') = \tilde{B} \left[ \theta(a - r_{<}) + \left( \alpha \frac{e^{-\kappa r_{<}}}{r_{<}} + \beta \frac{e^{\kappa r_{<}}}{r_{<}} \right) \theta(r_{<} - a) \right] \\ \times \left[ \left( \frac{\tilde{\gamma}}{r_{>}} + 1 \right) \theta(a - r_{>}) + \left( \tilde{\alpha} \frac{e^{-\kappa r_{>}}}{r_{>}} + \tilde{\beta} \frac{e^{\kappa r_{>}}}{r_{>}} \right) \theta(r_{>} - a) \right], \quad (3.11)$$

where

$$\alpha = \frac{e^{\kappa a}(\kappa a - 1)}{2\kappa} \quad (3.12)$$

$$\beta = \frac{e^{-\kappa a}(\kappa a + 1)}{2\kappa} \quad (3.13)$$

$$\tilde{\gamma} = \frac{1}{\kappa} \left[ \frac{e^{2\kappa R - \kappa a}(\kappa R - 1)(\kappa a + 1) - e^{\kappa a}(\kappa a - 1)(\kappa R + 1)}{[e^{\kappa a}(\kappa R + 1) - e^{2\kappa R - \kappa a}(\kappa R - 1)]} \right] \quad (3.14)$$

$$\tilde{\alpha} = \frac{1}{\kappa} \frac{e^{2\kappa R}(\kappa R - 1)}{[e^{\kappa a}(\kappa R + 1) - e^{2\kappa R - \kappa a}(\kappa R - 1)]} \quad (3.15)$$

$$\tilde{\beta} = \frac{1}{\kappa} \frac{(\kappa R + 1)}{[e^{\kappa a}(\kappa R + 1) - e^{2\kappa R - \kappa a}(\kappa R - 1)]} \quad (3.16)$$

$$\tilde{B} = \frac{1}{\tilde{\gamma}} \quad (3.17)$$

and  $r_{>}(r_{<})$  denotes the larger (smaller) one of  $r$  and  $r'$ . The full Green's function for the  $l = 0$  sector is thus

$$G(r, r') = g_0(r, r') Y_{00}^* Y_{00} \quad (3.18) \\ = \frac{\tilde{B}}{4\pi} \left[ \theta(a - r_{<}) + \left( \alpha \frac{e^{-\kappa r_{<}}}{r_{<}} + \beta \frac{e^{\kappa r_{<}}}{r_{<}} \right) \theta(r_{<} - a) \right] \\ \times \left[ \left( \frac{\tilde{\gamma}}{r_{>}} + 1 \right) \theta(a - r_{>}) + \left( \tilde{\alpha} \frac{e^{-\kappa r_{>}}}{r_{>}} + \tilde{\beta} \frac{e^{\kappa r_{>}}}{r_{>}} \right) \theta(r_{>} - a) \right]. \quad (3.19)$$

---

<sup>8</sup>See Appendix B for details.

### 3.2 Classical Solution

The electric potential is

$$\begin{aligned}
\phi_{elec}(\vec{r}) &= -i\phi_{SP}(\vec{r}) \\
&= -i^2 4\pi\ell_B \int d\vec{r}' G(\vec{r}, \vec{r}') \rho_m(\vec{r}') \\
&= \frac{4\pi\ell_B \tilde{B} z_m}{4\pi} \int_0^{2\pi} d\phi \int_0^\pi \sin\theta \int_0^R \frac{\delta(r')}{4\pi r'^2} r'^2 g(r, r') dr' \\
&= \ell_B \tilde{B} z_m \left[ \left( \frac{\tilde{\gamma}}{r_{>}} + 1 \right) \theta(a - r_{>}) + \left( \tilde{\alpha} \frac{e^{-\kappa r_{>}}}{r_{>}} + \tilde{\beta} \frac{e^{\kappa r_{>}}}{r_{>}} \right) \theta(r_{>} - a) \right] \\
&\times \int_0^R \left[ \theta(a - r_{<}) + \left( \alpha \frac{e^{-\kappa r_{<}}}{r_{<}} + \beta \frac{e^{\kappa r_{<}}}{r_{<}} \right) \theta(r_{<} - a) \right] \delta(r') dr' \\
&= \ell_B \tilde{B} z_m \left[ \left( \frac{\tilde{\gamma}}{r} + 1 \right) \theta(a - r) + \left( \tilde{\alpha} \frac{e^{-\kappa r}}{r} + \tilde{\beta} \frac{e^{\kappa r}}{r} \right) \theta(r - a) \right]. \tag{3.20}
\end{aligned}$$

The integration above is only done over  $r_{<}$  due to the delta-function source.

To check our results we take the  $R \rightarrow \infty$  limit, and find that the prefactors above reduce to

$$\alpha_\infty = \frac{e^{\kappa a}(\kappa a - 1)}{2\kappa} \tag{3.21}$$

$$\beta_\infty = \frac{e^{-\kappa a}(\kappa a + 1)}{2\kappa} \tag{3.22}$$

$$\tilde{\gamma}_\infty = -\frac{\kappa a + 1}{\kappa} \tag{3.23}$$

$$\tilde{\alpha}_\infty = -\frac{e^{\kappa a}}{\kappa} \tag{3.24}$$

$$\tilde{\beta}_\infty = 0 \tag{3.25}$$

$$\tilde{B}_\infty = \frac{1}{\tilde{\gamma}} = -\frac{\kappa}{\kappa a + 1}, \tag{3.26}$$

such that

$$\phi_{elec}(r) = 4\pi\ell_B z_m \left( \left[ \frac{1}{r} - \frac{\kappa}{\kappa a + 1} \right] \theta(a - r) + \left[ \left( \frac{e^{\kappa a}}{\kappa a + 1} \right) \frac{e^{-\kappa r}}{r} \right] \theta(r - a) \right), \tag{3.27}$$

which is the DLVO theory result [5].

### 3.3 Mean-field contribution to the free energy

In this section we will calculate the first term in eq.(3.2). We denote this term by  $F_{elec}$ . Thus,

$$\begin{aligned}
F_{elec} &= k_B T \frac{4\pi\ell_B}{2} \int d\vec{x} \int d\vec{y} \rho_m(\vec{x}) G(\vec{y}, \vec{x}) \rho_m(\vec{y}) \\
&= \frac{1}{2} k_B T \int d\vec{x} \phi_{elec}(\vec{x}) \rho_m(\vec{x}) \\
&= \frac{1}{2} k_B T \frac{4\pi\ell_B \tilde{B} z_m^2}{4\pi} \int_0^{2\pi} d\phi \int_0^\pi \sin\theta \int_0^R r^2 \frac{\delta(r)}{4\pi r^2} \left[ \left( \frac{\tilde{\gamma}}{r} + 1 \right) \theta(a-r) \right. \\
&\quad \left. + \left( \tilde{\alpha} \frac{e^{-\kappa r}}{r} + \tilde{\beta} \frac{e^{\kappa r}}{r} \right) \theta(r-a) \right] dr \\
&= \frac{1}{2} k_B T \ell_B \tilde{B} z_m^2 \int_0^R \left( \frac{\tilde{\gamma}}{r} + 1 \right) \delta(r) dr. \tag{3.28}
\end{aligned}$$

Formally this integral diverges due to the first term,  $\int_0^R \left( \frac{\tilde{\gamma}}{r} \right) \delta(r) dr$ . This term, however, represents the self-energy of the macro-ion and has to be subtracted. The resulting expression for the energetic part of the free energy is thus

$$\begin{aligned}
k_B T \frac{\ell_B \tilde{B} z_m^2}{2} \int_0^R \delta(r) dr &= k_B T \frac{\ell_B \tilde{B} z_m^2}{2} \\
&= \frac{1}{2} \frac{Q_m^2 \tilde{B}}{4\pi\epsilon_0}, \tag{3.29}
\end{aligned}$$

where we have used the definition of the Bjerrum length and the fact that  $Q_m = ez_m$ . This represents the electrostatic energy of the counterions and the macro-ion.

Subtracting the reference system mean-field free energy thus gives

$$\Delta F_{elec} = \frac{1}{2} \frac{Q_m^2}{4\pi\epsilon_0} (\tilde{B} - \tilde{B}_0), \tag{3.30}$$

where the subscript in  $B_0$  represents the reference system.

Let us again check whether this result is correct in the  $R \rightarrow \infty$  limit. In this case the energetic part of the free energy,  $F_{elec}$ , reduces to

$$F_{elec} = -\frac{1}{2} \frac{Q_m^2}{4\pi\epsilon_0} \left( \frac{\kappa}{\kappa a + 1} \right) \tag{3.31}$$

$$= -\frac{1}{2} \frac{Q_m^2}{4\pi\epsilon_0} \left( \frac{1}{a + \ell_{DH}} \right) \tag{3.32}$$

where  $\ell_{\text{DH}} = \frac{1}{\kappa}$  is the Debye screening length. This is the electrostatic energy due to the interaction between the macro-ion and the counterions [52, 5]. This makes sense since the counterions arrange themselves in a cloud (that neutralises the macro-ion charge) around the macro-ion at an average distance  $\ell_{\text{DH}}$  from the macro-ion surface. They are thus effectively an average distance of  $a + \ell_{\text{DH}}$  from the charge on the macro-ion. This expression for the electrostatic energy is simply the average electrostatic energy of two charges, each of valence  $z_m$ , at a distance  $a + \ell_{\text{DH}}$  from each other.

## CHAPTER 4

### Free energy: fluctuations

The fluctuation contribution is in general quite difficult to compute since it involves the calculation of a functional determinant. Since results of these types of calculations generally diverge, some regularisation and renormalisation schemes have to be implemented to ensure that physically sensible results are obtained. In our current calculation the operator always has bound states, stemming from the fact that the system volume is finite and we will present a technique for treating both bound states and scattering states within a unified framework. In this chapter we show how to calculate the determinant of the operator  $(-\nabla^2 + \kappa^2\mu)$  by making use of the zeta-function technique [49, 50].

Let us first comment on the calculation of the determinant. The problem we are considering in computing the determinant is equivalent to that of a particle subject to a finite square-well potential confined within a larger finite volume. One way of approaching this is to consider the larger confining volume as an additional background potential that the particle feels. A technical complication arises from the fact that it is not the wavefunction of the particle that must become zero outside the confining volume, but rather its derivative (the electrostatic considerations determine this).

Implementing this scheme of an additional background potential is difficult, and we therefore consider the simpler alternative of replacing the background potential by the appropriate boundary conditions on the eigenfunctions and solving the eigenvalue problem subject to these boundary conditions. We shall comment on the appropriateness of the boundary conditions later when we discuss the regularisation procedure in section 4.2.2.

Before we compute the determinant, we first give a general outline of the zeta-function technique.

#### 4.1 Zeta-function technique

In applications one is often interested in determining  $\ln \det \hat{A}$ . The determinant of the operator is defined as

$$\det \hat{A} = \prod_n \lambda_n^2, \quad (4.1)$$

where the  $\lambda_n^2$  are the eigenvalues. The generalised zeta function is defined as

$$\begin{aligned}\zeta(s) &= \sum_n \lambda_n^{-2s} \\ &= \sum_n e^{-2s \ln \lambda_n}.\end{aligned}\quad (4.2)$$

This definition is correct as long as the series converges. Beyond that, the zeta-function has to be defined by analytic continuation [53]. Thus,

$$\begin{aligned}\zeta'(0) &= - \sum_n (\ln \lambda_n^2) e^{-2s \ln \lambda_n} \Big|_{s=0} \\ &= - \sum_n \ln \lambda_n^2 \\ &\equiv - \ln \det \hat{A}.\end{aligned}\quad (4.3)$$

We will show how to rewrite the zeta function in terms of a contour integral.

To obtain the eigenvalues we have to solve the equation

$$\hat{A}\psi_n = \lambda_n^2 \psi_n \quad (4.4)$$

subject to the appropriate boundary conditions. Often solving the eigenvalues of this equation can be mapped onto the algebraic problem of finding the zeros of an entire function as explained in [50]. For the moment the precise nature of this function and the way it is obtained is irrelevant. Let us simply assume the existence of such a function, denoted  $F(\lambda)$ , from which we can determine the eigenvalues by solving  $F(\lambda_n) = 0$ . The logarithmic derivative of  $F$ ,

$$\frac{d}{d\lambda} \ln F(\lambda) = \frac{F'(\lambda)}{F(\lambda)}, \quad (4.5)$$

has poles at the eigenvalues. By expanding the logarithmic derivative around the eigenvalues and for  $F'(\lambda_n) \neq 0$  we obtain

$$\begin{aligned}\frac{F'(\lambda)}{F(\lambda)} &= \frac{F'(\lambda_n) + (\lambda - \lambda_n)F''(\lambda_n) + \dots}{(\lambda - \lambda_n)F'(\lambda_n) + \frac{1}{2}(\lambda - \lambda_n)^2 F''(\lambda_n) + \dots} \\ &= \frac{1}{\lambda - \lambda_n} \left( \frac{F'(\lambda_n) + (\lambda - \lambda_n)F''(\lambda_n) + \dots}{F'(\lambda_n) + \frac{1}{2}(\lambda - \lambda_n)^2 F''(\lambda_n) + \dots} \right).\end{aligned}\quad (4.6)$$

We can now use the residue theorem to write the zeta-function as a contour integral.

Consider

$$f(\lambda) = \lambda^{-2s} \frac{F'(\lambda)}{F(\lambda)}. \quad (4.7)$$

We know that

$$\int_{\gamma} d\lambda f(\lambda) = 2\pi i \sum_n \text{Res}[f(\lambda_n)], \quad (4.8)$$

where  $\gamma$  is a contour that encloses all the  $\lambda_n$ , and

$$\begin{aligned} \text{Res}[f(\lambda_n)] &= \lim_{\lambda \rightarrow \lambda_n} (\lambda - \lambda_n) f(\lambda) \\ &= \lambda_n^{-2s}. \end{aligned} \quad (4.9)$$

Thus we finally have

$$\begin{aligned} \zeta(s) &= \sum_n \lambda_n^{-2s} \\ &= \frac{1}{2\pi i} \int_{\gamma} d\lambda \lambda^{-2s} \frac{d}{d\lambda} \ln F(\lambda). \end{aligned} \quad (4.10)$$

The zeta-function as it is given above is not defined for  $s = 0$ .

In physical applications one is interested in calculating the ratio of two determinants.

This amounts to calculating the difference between two zeta functions. Let us denote the zeta-function for our reference system by

$$\zeta_0(s) = \frac{1}{2\pi i} \int_{\gamma} d\lambda \lambda^{-2s} \frac{d}{d\lambda} \ln F_0(\lambda). \quad (4.11)$$

Then the difference between two zeta-functions is

$$\bar{\zeta}(s) = \zeta(s) - \zeta_0(s) = \frac{1}{2\pi i} \int_{\gamma} d\lambda \lambda^{-2s} \frac{d}{d\lambda} \ln \frac{F(\lambda)}{F_0(\lambda)}. \quad (4.12)$$

We now deform the contour to the imaginary axis. We have to bear in mind that there is a branch cut for  $\lambda^{-2s}$ , that is defined to be on the negative real axis. Deforming the contour to the imaginary axis, we get the following contribution for the positive imaginary axis;

$$\bar{\zeta}^+(s) = \zeta^+(s) - \zeta_0^+(s) = -\frac{1}{2\pi i} e^{-i\pi s} \int_0^{\infty} d\lambda \lambda^{-2s} \frac{d}{d\lambda} \ln \frac{F(i\lambda)}{F_0(i\lambda)}. \quad (4.13)$$

Likewise, for the negative imaginary axis we get the contribution

$$\bar{\zeta}^-(s) = \zeta^-(s) - \zeta_0^-(s) = \frac{1}{2\pi i} e^{i\pi s} \int_0^\infty d\lambda \lambda^{-2s} \frac{d}{d\lambda} \ln \frac{F(-i\lambda)}{F_0(-i\lambda)}. \quad (4.14)$$

Adding these two contributions and using the fact that  $F(-i\lambda) = F(i\lambda)$  we find that the zeta-function representation becomes

$$\bar{\zeta}(s) = \frac{\sin(\pi s)}{\pi} \int_0^\infty d\lambda \lambda^{-2s} \frac{d}{d\lambda} \ln \frac{F(i\lambda)}{F_0(i\lambda)}. \quad (4.15)$$

As  $|\lambda| \rightarrow \infty$ , we should at least have that

$$\frac{d}{d\lambda} \ln \frac{F(i\lambda)}{F_0(i\lambda)} \sim \frac{1}{\lambda^2}. \quad (4.16)$$

Together with the behaviour of  $\frac{d}{d\lambda} \ln \frac{F(i\lambda)}{F_0(i\lambda)}$  at the lower integration limit, this will ensure that the representation is valid for  $-\frac{1}{2} < s < \frac{1}{2}$ , which makes the zeta-function well defined at  $s = 0$ .

We have that

$$\begin{aligned} \bar{\zeta}'(0) &= \left( \cos(\pi s) \int_0^\infty d\lambda \lambda^{-2s} \frac{d}{d\lambda} \ln \frac{F(i\lambda)}{F_0(i\lambda)} \right) \Big|_{s=0} - \left( \frac{\sin(\pi s)}{\pi} \int_0^\infty d\lambda \lambda^{-2s} \ln \lambda \frac{d}{d\lambda} \ln \frac{F(i\lambda)}{F_0(i\lambda)} \right) \Big|_{s=0} \\ &= \int_0^\infty d\lambda \frac{d}{d\lambda} \ln \frac{F(i\lambda)}{F_0(i\lambda)} \\ &= -\ln \frac{F(0)}{F_0(0)}. \end{aligned} \quad (4.17)$$

## 4.2 Fluctuation contribution to free energy

We remind the reader that we compute the free energy of the system as a function of the macro-ion radius within a fixed confining radius and choose as our reference point for the free energy a macro-ion with a fixed radius  $a_0$ .

For the free energy calculation we consider the eigenvalue problem

$$(-\nabla^2 + \kappa^2 \mu) \psi_n = \lambda_n^2 \psi_n. \quad (4.18)$$

This is similar to solving the Schrödinger equation with the square-well potential in Quantum Mechanics, but with the well-depth  $\kappa^2$ . In our free energy calculation we are changing the macro-ion radius, which amounts to changing the radius of the well. We



note, however, that since

$$\kappa^2 = 4\pi l_B n_c z_c^2 \quad (4.19)$$

$$= \frac{3l_B z_m z_c^2}{R^3 - a^3}, \quad (4.20)$$

the depth also changes as we change the radius.

Performing a separation of variables, we can write the eigenfunctions as

$$\psi(r, \theta, \phi) = R_l(r) Y_{lm}(\theta, \phi). \quad (4.21)$$

The eigenvalues for each  $l$ -channel are then determined by the radial equation,

$$\frac{1}{r} \frac{d^2}{dr^2} [r R_l(r)] - \left[ \frac{l(l+1)}{r^2} + \kappa^2 \mu \right] R_l(r) = \lambda R_l(r), \quad (4.22)$$

subject to the boundary conditions,

$$R_l(k_1 a) = R_l(k_2 a) \quad (4.23)$$

$$\left. \frac{dR_l(k_1 r)}{dr} \right|_{r=a} = \left. \frac{dR_l(k_2 r)}{dr} \right|_{r=a} \quad (4.24)$$

$$\left. \frac{dR_l(k_2 r)}{dr} \right|_{r=R} = 0. \quad (4.25)$$

In the boundary conditions above  $k_1^2 = \lambda_n^2$  and  $k_2^2 = \lambda_n^2 - \kappa^2$ . The square-well potential has both bound-states and scattering states. We will comment below on how one can obtain the eigenvalues of both these types of states from a single equation.

The general solution to the radial equation is

$$R_l(r) = A j_l(k_1 r) \theta(a - r) + [B j_l(k_2 r) + C n_l(k_2 r)] \theta(r - a), \quad (4.26)$$

where  $j_l$  and  $n_l$  are the spherical Bessel and Neumann functions respectively. It is important to note that since the counterions occupy a finite volume, the exponentially growing and decaying solutions in the region  $a < r < R$  are both allowed for bound states for which  $k_2^2 < 0$ . Hence (4.26) is indeed the most general solution capturing both the scattering and bound states, provided that we allow  $k_2^2 < 0$ . Using the solution

(4.26) with the boundary conditions gives the following three equations:

$$Aj_l(k_1a) - Bj_l(k_2a) - Cn_l(k_2a) = 0 \quad (4.27)$$

$$Ak_1j'_l(k_1a) - Bk_2j'_l(k_2a) - Ck_2n'_l(k_2a) = 0 \quad (4.28)$$

$$Bk_2j'_l(k_2R) - Ck_2n'_l(k_2R) = 0. \quad (4.29)$$

We can rewrite this in matrix form

$$\begin{pmatrix} j_l(k_1a) & j_l(k_2a) & n_l(k_2a) \\ k_1j'_l(k_1a) & -k_2j'_l(k_2a) & -k_2n'_l(k_2a) \\ 0 & -j'_l(k_2R) & -n'_l(k_2R) \end{pmatrix} \begin{pmatrix} A \\ B \\ C \end{pmatrix} = \begin{pmatrix} 0 \\ 0 \\ 0 \end{pmatrix}.$$

This equation has non-trivial solutions if and only if the determinant of the  $3 \times 3$  matrix is zero. That is,

$$\begin{aligned} 0 &= k_2j_l(k_1a)[n'_l(k_2a)j'_l(k_2R) - j'_l(k_2a)n'_l(k_2R)] \\ &+ k_1j'_l(k_1a)[j_l(k_2a)n'_l(k_2R) - n_l(k_2a)j'_l(k_2R)]. \end{aligned} \quad (4.30)$$

The real valued  $k_1$  that solves this equation will give us eigenvalues for each  $l$ -channel. Therefore, the function  $F_l$  that determines the eigenvalues for each  $l$ -channel is given by

$$\begin{aligned} F_l(k_1) &= k_2Rj_l(k_1a)[n'_l(k_2a)j'_l(k_2R) - j'_l(k_2a)n'_l(k_2R)] \\ &+ k_1Rj'_l(k_1a)[j_l(k_2a)n'_l(k_2R) - n_l(k_2a)j'_l(k_2R)]. \end{aligned} \quad (4.31)$$

The bound state eigenvalues are those for which  $\lambda_n^2 < \kappa^2$  (or  $k_1^2 < \kappa^2$ ) and the scattering states those for which  $\lambda_n^2 > \kappa^2$  (or  $k_1^2 > \kappa^2$ ). Note that for real valued  $k_1$  all eigenvalues are positive as one would expect for a potential bounded below by zero.

For convenience we consider the dimensionless quantity  $\chi = k_1R$ . We note that the following relations hold.

$$\begin{aligned} k_1a &= k_1Rx \\ k_2a &= k_2Rx \\ \kappa a &= \kappa Rx, \end{aligned}$$

where  $x = \frac{a}{R}$  and  $\kappa a = \sqrt{3 \frac{\ell_B}{R} \frac{z_m z_c x^2}{(1-x^3)}}$ . These relations will help to simplify the rewriting of

certain expressions.

Eq.(4.31) is valid for each  $l$ -channel. One can compute the determinant for each channel separately (a 1-dimensional problem) and the total determinant is then simply the product of all these 1-dimensional determinants.

As mentioned, the zeros of  $F$  determine the eigenvalues of the operator, but from the calculations it emerges that  $F$  has a singularity at  $\chi = \kappa R$ . This does not represent an actual eigenvalue of the operator, and its contribution has to be subtracted when performing the contour integral. It can be shown that the residue of  $\frac{d}{d\chi} \ln F(\chi)$  is equal to -1 at  $\chi = \kappa R$ . We thus have

$$\zeta(s) = \frac{1}{2\pi i} \int_{\gamma} d\chi \chi^{-2s} \frac{d}{d\chi} \ln F_l(\chi) + (\kappa R)^{-2s} \quad (4.32)$$

after the contribution at  $\chi = \kappa R$  is subtracted. That this is correct is confirmed by the agreement between the analytical results and explicit numerical calculation of the ratio of determinants as discussed in the following subsection.

Deforming the contour to the imaginary axis the zeta-function representation for the ratio of determinants becomes

$$\bar{\zeta}(s) = \zeta(s) - \zeta_0(s) = \frac{\sin \pi s}{\pi} \int_0^{\infty} d\chi \chi^{-2s} \frac{d}{d\chi} \ln \left( \frac{F_l(i\chi)}{F_l^{(0)}(i\chi)} \right) + (\kappa R)^{-2s} - (\kappa_0 R)^{-2s}, \quad (4.33)$$

where  $\kappa_0^2$  is the well-depth associated with our reference system.

We still have to consider the asymptotic behaviour of  $\frac{d}{d\chi} \ln \frac{F_l(i\chi)}{F_l^{(0)}(i\chi)}$  as  $|\chi| \rightarrow \infty$ . We find that

$$\frac{F_l(i\chi)}{F_l^{(0)}(i\chi)} \simeq \left( \frac{x_0}{x} \right)^2 \left( 1 + \frac{\tilde{C}}{\chi} + \dots \right). \quad (4.34)$$

As  $|\chi| \rightarrow 0$ , the integrand behaves as  $\chi^{-2s}$ . The representation in eq.(4.33) is thus valid for  $-\frac{1}{2} < s < \frac{1}{2}$ . We finally have that for each  $l$ -channel

$$\begin{aligned} \ln \left( \frac{\det(-\nabla^2 + \kappa^2 \mu)}{\det(-\nabla^2 + \kappa_0^2 \mu_0)} \right)_l &= -\zeta'(0) \\ &= \int_0^{\infty} d\chi \frac{d}{d\chi} \ln \left( \frac{F_l(i\chi)}{F_l^{(0)}(i\chi)} \right) + \ln(\kappa R)^2 - \ln(\kappa_0 R)^2 \\ &= \ln \left( \frac{F_l(0)}{F_l^{(0)}(0)} \right) - \ln \left( \frac{x_0}{x} \right)^2 + \ln \left( \frac{\kappa}{\kappa_0} \right)^2. \end{aligned} \quad (4.35)$$

The contribution from the upper integration limit is a direct consequence of eq.(4.34). The result in eq.(4.35) is dependent on the potential, in this case  $\kappa\mu(\vec{x})$ , satisfying the same conditions as do the potentials studied by Dunne and Kirsten in [48]. We have not analytically verified whether the finiteness of the confining volume influence these conditions, however, the explicit numerical verification of the results in eq.(4.35) indicate that the necessary conditions on the potential are satisfied, and therefore the assumed analytical properties of the function  $F$  hold.

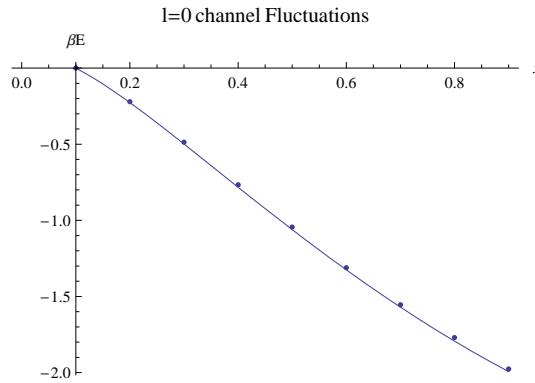
#### 4.2.1 Numerical verification of the 1-dimensional determinants

The analytical results obtained in the previous subsection were verified numerically for individual  $l$ -channels. In this section we briefly describe the numerical procedure and show some results. All of the numerical work was performed using *Mathematica*. As mentioned above, the eigenvalues of the operator  $(-\nabla^2 + \kappa^2\mu)$  are determined by the zeros of the function  $F$ . We present a simple numerical scheme to approximate these zeros. It consists of finding the points where the function  $F$  changes sign. At those points, it goes through zero and we have the eigenvalues. The basic procedure is as follows: we consider a finite interval  $[k_{init}, k_{final}]$  that is divided it into smaller subintervals of equal length,  $\Delta k$ . The number of intervals,  $N$ , is determined by the width of the individual intervals, that is  $N = \frac{k_{final} - k_{init}}{\Delta k}$ , with  $k_{init}$  and  $k_{final}$  the initial and final points respectively. If the function changes sign in the interval  $[k_j, k_{j+1}]$ , the value for the zero is taken to be the midpoint of the interval, i.e.  $k_j + \frac{\Delta k}{2}$ . One of course has to be careful not to miss any of the zeroes. This is done by subdividing the intervals  $\Delta k$  again and repeating the procedure.

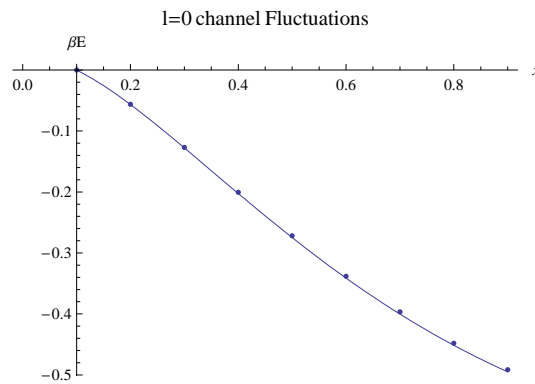
Since we are interested in the ratio of two determinants, we perform the procedure for the reference system also. We then take the product of the eigenvalues for each operator, and finally the ratio of the two products. A factor that influences the accuracy of the numerical calculation is the size of the interval  $[k_{init}, k_{final}]$  for the two determinants. The larger the interval, the more accurate the results will be since one includes more of the eigenvalues of the operators. The choice of the interval length is determined by the system parameters. For shallow potential wells, one can choose the interval to be relatively small. Since we are considering the ratio of two determinants of two similar operators, one expects that the very large eigenvalues of both operators should be the same, and these will eventually cancel out when taking the ratio. For deeper wells, we

have to include more eigenvalues since more eigenvalues are shifted relative to the reference system, and hence the cancellation of eigenvalues only occurs at larger eigenvalues. In practice one has to test where the cancellation starts and then choose  $k_{final}$  accordingly.

The figures represent some results for two channels only and arbitrary parameter values. We have tested this extensively for a wide range of parameter values and many different  $\ell$ -channels.

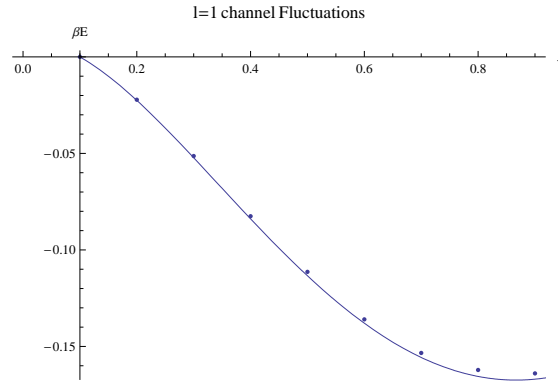


**Figure 4.1:** Plot of the comparison of the numerical and analytical results for the fluctuation contribution for the  $l=0$  channel for  $\frac{\ell_B}{R} = \frac{1}{10}$ . The solid line represents the analytical result and the dots the data points of the numerical calculation.



**Figure 4.2:** Plot of the comparison of the numerical and analytical results for the fluctuation contribution for the  $l=0$  channel for  $\frac{\ell_B}{R} = \frac{1}{50}$ . The solid line represents the analytical result and the dots the data points of the numerical calculation.

We see that the direct numerical computation and the analytical results agree very well.

4. Free energy: fluctuations

**Figure 4.3:** Plot of the comparison of the numerical and analytical results for the fluctuation contribution for the  $l=1$  channel for  $\frac{\ell_B}{R} = \frac{1}{50}$ . The solid line represents the analytical result and the dots the data points of the numerical calculation.

## 4.2.2 Regularisation

The expression for the ratio of determinants is valid for each  $l$ -sector. To obtain the full ratio of determinants, we have to perform the summation over the  $l$ -channels. Thus the total ratio is given by

$$\ln \left( \frac{\det(-\nabla^2 + \kappa^2 \mu)}{\det(-\nabla^2 + \kappa_0^2 \mu_0)} \right) = \sum_{l=0}^{\infty} (2l+1) \ln \left( \frac{\det(-\nabla^2 + \kappa^2 \mu)}{\det(-\nabla^2 + \kappa_0^2 \mu_0)} \right)_l, \quad (4.36)$$

where  $(2l+1)$  is the degeneracy in each channel. This series is divergent and we have to find some way of regularising it. We propose to introduce a cut-off,  $L$ , in the series and thus write,

$$\ln \left( \frac{\det(-\nabla^2 + \kappa^2 \mu)}{\det(-\nabla^2 + \kappa_0^2 \mu_0)} \right)_{reg} = \sum_{l=0}^L (2l+1) \ln \left( \frac{\det(-\nabla^2 + \kappa^2 \mu)}{\det(-\nabla^2 + \kappa_0^2 \mu_0)} \right)_l. \quad (4.37)$$

The question remains as to what is a sensible value for  $L$ . The origin of the divergence lies in the fact that we consider the counterions as point-particles, whereas in reality they have a finite size. The counterion size sets the smallest length scale of the problem, but the large scale physics should be independent of it, and indeed we find that this is so. We now also comment on the appropriateness of the boundary condition in eq.(4.25). It could be argued that the boundary condition eq.(4.25) is unrealistic, but our assumption of point-like counterions is also an idealisation, since as just mentioned above, there exists a smallest length scale set by the counterion size. The choice of the boundary

condition seems consistent within the approximation of point-like counterions.

In order to deal with this divergence we adopt the strategy of assigning a finite size to the counterions, compute the free energy of the counterions in the volume available in the limit  $T \rightarrow \infty$ . We know in that limit the free energy is entirely entropic. The particles are essentially non-interacting and the free energy can be calculated exactly. We then consider the regularised fluctuation calculation and see how each of the  $l$ -sector determinants behaves in the  $T \rightarrow \infty$  limit. We can then determine where to terminate the series by matching the entropy computed for the finite size counterions with the regularised calculation. This will give a cut-off for the summation in terms of physical parameters of the system.

Assume the counterions have a radius  $r_c$ . The total number of counterions that can be accommodated is the total volume available to the counterions divided by the volume of a single counterion. That is,

$$N = \frac{V_s - V_m}{V_c} = \frac{R^3 - a^3}{r_c^3}, \quad (4.38)$$

with  $V_s$  the system volume,  $V_m$  the macro-ion volume and  $V_c$  the volume of individual counterions. In the  $T \rightarrow \infty$  limit the distribution of the counterions over the available slots is energetically the same, and we can estimate the entropy by simply computing the number of arrangements. As our system contains  $N_c$  identical counterions this is simply

$$\Omega = \frac{N!}{(N - N_c)!N_c!}. \quad (4.39)$$

Therefore,

$$\ln \Omega \simeq N \ln N - (N - N_c) \ln (N - N_c) - N_c \ln N_c, \quad (4.40)$$

where we have made use of Stirling's approximation. When computing the partition function we linearised the action, which is equivalent to taking the low density limit. We make the same approximation here, i.e. we take  $N_c \ll N$ . Thus,

$$\begin{aligned} & N \ln N - (N - N_c) \ln (N - N_c) - N_c \ln N_c \\ &= N \ln N - (N - N_c) \ln \left[ N \left( 1 - \frac{N_c}{N} \right) \right] - N_c \ln N_c \\ &= N_c \ln N + N_c - N_c \ln N_c, \end{aligned} \quad (4.41)$$

where we have expanded  $\ln(1 - \frac{N_c}{N})$  to leading order. We again have to subtract the free energy of the reference system with fixed macro-ion size. We denote the total number of

counterions that can be accommodated in the reference system by  $\tilde{N}$ . The number of counterions in both systems is the same, therefore we have that the difference in free energy is

$$\begin{aligned}\beta\Delta F &= -\ln\left(\frac{\Omega}{\tilde{\Omega}}\right) \\ &= -N_c \ln\left(\frac{N}{\tilde{N}}\right) \\ &= N_c \ln\left(\frac{R^3 - a_0^3}{R^3 - a^3}\right).\end{aligned}\quad (4.42)$$

When taking the  $T \rightarrow \infty$  limit in eq.(4.35), one finds it reduces to

$$\ln\left(\frac{\det(-\nabla^2 + \kappa^2\mu)}{\det(-\nabla^2 + \kappa_0^2\mu_0)}\right)_l = \ln\left(\frac{\kappa}{\kappa_0}\right)^2 = \ln\left(\frac{R^3 - a_0^3}{R^3 - a^3}\right).\quad (4.43)$$

This is simply the ideal gas entropy difference (compare eq.(4.42)) for the particular  $l$ -channel. We see that by taking the limit we have identified the terms in the fluctuation contribution that encode the correlations between the ions, i.e. the first two terms in eq.(4.35). In the introduction to this work we mentioned this question of how to encode the counterion correlations. We see here that we have an explicit expression for the correlation contribution. In the  $T \rightarrow \infty$  limit the regularised summation therefore becomes

$$\begin{aligned}\sum_{l=0}^L (2l+1) \ln\left(\frac{\det(-\nabla^2 + \kappa^2\mu)}{\det(-\nabla^2 + \kappa_0^2\mu_0)}\right)_l &= \sum_{l=0}^L (2l+1) \ln\left(\frac{\kappa}{\kappa_0}\right)^2 \\ &= \sum_{l=0}^L (2l+1) \ln\left(\frac{R^3 - a_0^3}{R^3 - a^3}\right) \\ &= (L+1)^2 \ln\left(\frac{R^3 - a_0^3}{R^3 - a^3}\right).\end{aligned}\quad (4.44)$$

If we compare this to eq.(4.42), we see that

$$N_c = (L+1)^2.\quad (4.45)$$

Therefore,  $L = \sqrt{N_c} - 1$ . This provides us with a regularisation in terms of physical parameters since charge neutrality determines that  $N_c = \frac{zm}{z_c}$ . These values are fixed for the system under consideration.



For the case where salt is added to the solution, the regularisation proceeds in exactly the same manner as described above, except that we replace  $N_c$  everywhere with  $N_{ion} = N_c + N_+ + N_-$ . The prescription then becomes  $L = \sqrt{N_{ion}} - 1 = \sqrt{N_c + N_+ + N_-} - 1$ , where  $N_c, N_+$  and  $N_-$  are the number of counterions, positive salt ions and negative salt ions respectively. The regularisation prescription is again given in terms of physical parameters and is unambiguous for the system under consideration.

## CHAPTER 5

### Results and Conclusions

In the preceding chapters we have developed the formalism and found analytical expressions for the free energy of our system under consideration. In this chapter we present some results for the free energy calculation for various values of the parameters.

#### 5.1 Free energy

In figures (5.1) and (5.2) we plot the two contributions to the free energy separately to illustrate their respective behaviours at different temperatures as given by  $\ell_B/R$ . For figures (5.1) and (5.2) we used  $z_c = 1$  and  $z_m = 100$  for convenient representation. We

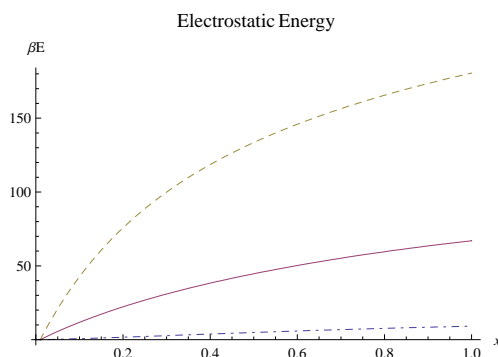


**Figure 5.1:** Electrostatic energy contribution to the free energy for various values of  $\ell_B/R$ . The dashed curve represent  $\ell_B/R = 1/50$ , the solid line  $\ell_B/R = 1/100$  and dot-dashed curve  $\ell_B/R = 1/500$ , respectively.

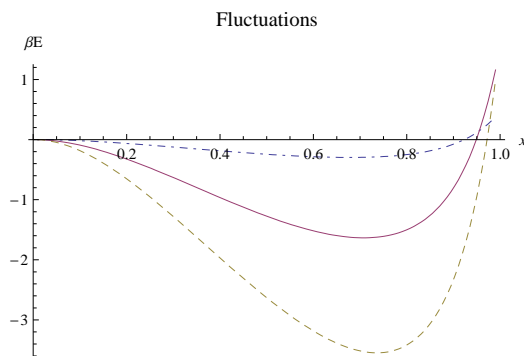


**Figure 5.2:** Fluctuation contribution to the free energy for various values of  $\ell_B/R$ . The dashed curve represent  $\ell_B/R = 1/50$ , the solid line  $\ell_B/R = 1/100$  and dot-dashed curve  $\ell_B/R = 1/500$ , respectively.

have verified that the qualitative trends remain unchanged with other values of these two parameters.

We see from the figures that the electrostatic (mean-field) contribution dominates the free energy and would favour a collapse of the macro-ion. The mean-field result makes sense since the counterions are attracted electrostatically to the macro-ion charge and expanding the macro-ion means performing work against the Coulomb attraction, by pushing out the counterions, which leads to an increase in the free energy.

The fluctuation contribution to the free energy at first decreases the free energy upon expansion of the macro-ion and then increases. This means that in a certain range of parameter space, expansion is favoured by the fluctuating part. The tendency to expand is indeed due to the correlation between counterions. That this is so can be seen by examining eq.(4.35) again. The fluctuation contribution per  $l$ -channel is

$$\ln \left( \frac{\det \left( -\nabla^2 + \kappa^2 \mu \right)}{\det \left( -\nabla^2 + \kappa_0^2 \mu_0 \right)} \right)_l = \ln \left( \frac{F_l(0)}{F_l^{(0)}(0)} \right) - \ln \left( \frac{x_o}{x} \right)^2 + \ln \left( \frac{\kappa}{\kappa_0} \right)^2.$$

The last term, the contribution of the ideal gas, is always positive. The reduction in the free energy, the negative contribution, is due to the first two terms, that are present only when the electrostatic interaction energy is non-zero. We have already seen that these two terms vanish when the limit  $T \rightarrow \infty$  is taken, i.e. when the electrostatic energy becomes zero when compared to the thermal energy. One can think of the fluctuating contribution in terms of the following physical picture: as the macro-ion initially expands, the correlations between the counterions are such that they utilise more of the available “surface area” to arrange themselves around the macro-ion. This continues until the loss in entropy of the counterions (with decreasing the available volume) starts resisting the expansion.

## 5.2 Role of the volume exclusion

The decrease in the free energy is a direct consequence of the volume exclusion in the field-theoretical formulation. Mathematically the decreasing free energy arises due to the presence of the bound states of the operator  $(-\nabla^2 + \kappa^2 \mu)$ . Increasing the macro-ion size, the “square well” becomes both deeper ( $\kappa^2$  increases) and broader and the bound state eigenvalues shift to a lower value relative to that of the shallower, narrower well.

That this is the case, can be seen from  $\kappa a = \sqrt{3 \frac{\ell_B}{R} \frac{z_m z_c x^2}{(1-x^3)}}$ . The lowering of the free energy

is directly related to this shift in the eigenvalues. However, it is only when the volume is explicitly excluded, and therefore the “square well mapping” applies, that this happens. If one were to model the excluded volume effect by some effective screening length that makes use of a “point-particle” approach to the macro-ion, one would not capture the non-perturbative effects. A point-particle approach to the macro-ion means setting our exclusion parameter  $\mu(\vec{x}) = 1$  throughout the entire system. This reduces the problem to the study of the ordinary Debye-Hückel theory.

It is easy to see that the effective Debye-Hückel approach will lead to a purely increasing fluctuation contribution by considering the following argument. Suppose we denote the effective screening length by  $\kappa^*$ . Increasing the macro-ion size means increasing the density and therefore increasing  $\kappa^*$ . This means that  $\kappa^* > \kappa_0^*$  (where the subscript again denotes our reference system) and therefore the eigenvalues of the operator, relative to the reference system, increase leading to an increase in the fluctuation contribution to the free energy in all of parameter space. This is represented in figure 5.3, where we plot the fluctuation contribution for the Debye-Hückel theory [54].

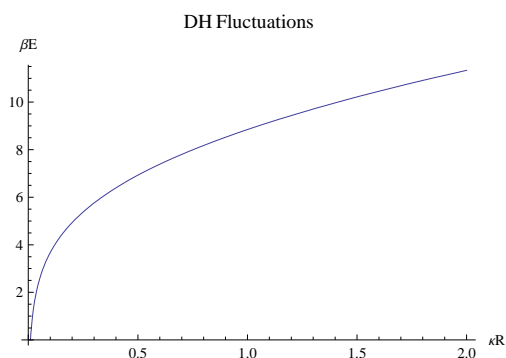


**Figure 5.3:** The fluctuation contribution for the ordinary Debye-Hückel theory as a function of the inverse screening length.

As clearly seen by the results, dealing with the exclusion of counterions from the macro-ion volume correctly and explicitly captures the correlation effects. The initial decrease of the fluctuation contribution of the free energy is only seen when making this mapping to the finite square well potential.

### 5.3 High temperature behaviour

Particular attention should be paid to the high temperature limit. In the previous chapter, when we developed the regularisation prescription, we saw that as  $T \rightarrow \infty$  the

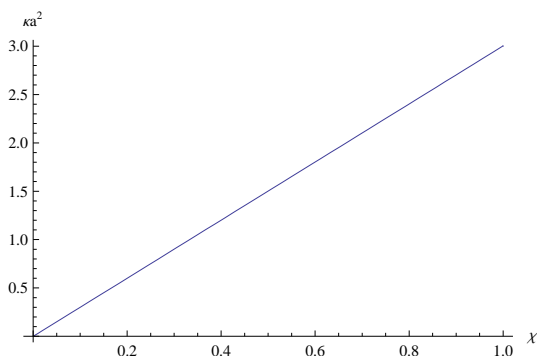


**Figure 5.4: Temperature dependence of the well depth. The figure shows  $(\kappa a)^2$  plotted as a function of  $\chi = \ell_B/R$ . Note that  $\ell_B$  is proportional to  $1/T$ .**

free energy becomes purely entropic (fluctuation contribution) and strictly positive. However, for finite  $T$ , the fluctuation contribution does not dominate the free energy at high  $T$  values. As figure 5.1 shows, the energetic contribution decreases with increasing temperature as expected, but the fluctuation contribution also becomes weaker. The reason for this weaker fluctuation contribution is that the well-depth in our square well mapping is temperature dependent. As the temperature increases, the well-depth decreases (see figure 5.4) and the bound states become “weaker”, and as a result the fluctuation contribution to the free energy becomes correspondingly smaller. Thus at finite temperature the fluctuation contribution is therefore not sufficient to induce a non-trivial minimum in the free energy.

It is also important to note that the entropy of the system is not contained in the fluctuation contribution alone. There is a subtle temperature dependence in the free energy and in order to obtain the entropy, one should take the derivative of the free energy with respect to temperature.

#### 5.4 Uniqueness of the regularisation prescription

We have constructed a method by which the fluctuation part of the free energy can be computed exactly. Our method handles both scattering and bound states simultaneously when computing the determinants. We also introduced a regularisation scheme in terms of purely physical parameters that are fixed for the system under consideration.

Although the cut-off in this regularisation scheme was determined by considering the  $T \rightarrow \infty$  limit, we do not expect it to exhibit a strong temperature dependence. The reason for this is that the cut-off is essentially determined by the length scale set by the

size of the counterions, which implicitly implies a cut-off in the summation over angular momentum sectors as one should not resolve a solid angle less than the one spanned by the counterions. The argument used here is a simple way of estimating this cut-off. Furthermore, note that in the low density limit the finite size of the counterions cancels out when subtracting the reference system free energy. We therefore certainly do not expect the quantitative results obtained above to depend much on the details of the regularisation scheme or the precise value of the cut-off.

### 5.5 What have we learnt?

We now return to the central objective of this dissertation, stated in section 1.6, and examine whether we are able to answer the questions posed there. We first restate it here for convenience. What role do the bound states play, specifically in the fluctuation contribution, and do they have some non-trivial effect on the physics of such a charged system? Could the role of the bound states in this simplified model provide some insight into the mechanism for like-charged attraction in the weak-coupling limit?

We have been able to identify the role the bound states play and list them below:

- (i) The bound states favour expansion of the macro-ion (attraction to the walls of the confining volume). The attraction to the wall is driven by the non-perturbative components. The field theory was linearised, yet non-trivial effects are still observed. Neglecting the non-linearities does not destroy all the non-trivial behaviour.
- (ii) The fluctuation contribution does not dominate the free energy at high, but finite, temperatures. This is certainly counter-intuitive, and is a direct consequence of the finite square well mapping.
- (iii) The fluctuation contribution alone is not strong enough to lead to an effective attraction between macro-ion and the walls of confining volume. Extrapolating to the effective attraction between two macro-ions, we suspect one will have to consider other mechanisms to explain this phenomenon in the weak-coupling limit.

One of the by-products of our analysis is the construction a novel regularisation scheme that enables one to write the cut-off completely in terms of physical parameters that are specified unambiguously.

## 5.6 Caveats

There are a number of caveats in the above computation that should be pointed out. Firstly, the low density (or equivalently high temperature) approximation, which allowed the linearisation, breaks down when the macro-ion size becomes comparable to the size of the system and the behaviour of the free energy obtained above is questionable in this limit. Another complication ignored above is the possibility of re-association of the counterions and macro-ion. One may expect that as the density of counterions is increased they may re-associate with the macro-ion and reduce the number of counterions in the solution and charge of the macro-ion. Related to this we have not allowed the possibility of a strong condensation of counterions on the surface of the macro-ion. This can, for instance, be captured by allowing a non-zero surface charge for the macro-ion, which can again be easily captured by a modification of the boundary condition eq.(2.10). Despite these possible refinements, we believe that the computation done here captures the essence of the physics as it is, apart from the linearisation approximation, essentially exact.

## 5.7 Outlook

One interesting variation on the problem considered in this dissertation would be to investigate what happens to the system if one were to explicitly break the spherical symmetry. At the moment the centers of the macro-ion and the confining volume coincide. The question is what would happen if one were to displace the macro-ion center slightly. Would the macro-ion be attracted to the side of the confining container, or would it simply return to its original position?

As mentioned in the introduction, the motivation for this calculational framework is understanding the effective interactions between macro-ions. The next step would be to extend and apply these calculational techniques to the case of multiple macro-ions. One way of doing this in a very approximate way would be to consider two such “cells” (spherically confined single macro-ion) and introduce some minimal coupling between them. A combination of this minimal coupling, together with the asymmetry mentioned in the previous paragraph, could be an interesting problem to investigate.

We have gained insight into the role of the various contributions to the free energy for the case of the linearised theory for spherical geometry. It would be interesting to perform a similar linearised calculation for the cylindrical geometry and compare it with

the exact non-linear results (the Poisson-Boltzmann equation can be solved analytically in this geometry) and see exactly what effect the non-linearities in the theory play. Finally, the techniques used here, and the insight gained from the analysis could be used as the starting point for approximations to more complex situations. These would typically be in the form of variational calculations where the current linearised theory could serve as the variational ansatz.



## APPENDIX A

### The zero-mode subtracted action

In the functional integral we replace  $\phi$  by  $\psi + \tilde{\phi}$ . We consider each of the terms in the Hamiltonian individually. We drop all arguments of the fields for now, except where there is possible confusion.

1.

$$\begin{aligned}
\int d\vec{x} \phi(\vec{x})(-\nabla^2)\phi(\vec{x}) &= -\frac{1}{2} \int (\psi + \tilde{\phi})(-\nabla^2)(\psi + \tilde{\phi}) \\
&= -\frac{1}{2} \int \psi(-\nabla^2)\psi - \frac{1}{2} \int \tilde{\phi}(-\nabla^2)\tilde{\phi} - \frac{1}{2} \int \tilde{\phi}(-\nabla^2)\psi - \frac{1}{2} \int \psi(-\nabla^2)\tilde{\phi} \\
&= -\frac{1}{2} \int \psi(-\nabla^2)\psi - \frac{1}{2} \int \tilde{\phi}(-\nabla^2)\psi
\end{aligned} \tag{A.1}$$

The second and the fourth terms in the second line above are zero since  $\tilde{\phi}$  is simply a number and therefore  $\nabla^2\tilde{\phi} = 0$ .

2.

$$\begin{aligned}
-iz_m \int d\vec{x} \delta(\vec{x})\phi &= -iz_m \int d\vec{x} (\psi + \tilde{\phi})\delta(\vec{x}) \\
&= -iz_m \int d\vec{x} \psi(\vec{x})\delta(\vec{x}) - iz_m \tilde{\phi} \int d\vec{x} \delta(\vec{x}) \\
&= -iz_m \int d\vec{x} \psi(\vec{x})\delta(\vec{x}) - iz_m \tilde{\phi}
\end{aligned} \tag{A.2}$$

3.

$$\begin{aligned}
\frac{1}{2} \frac{N}{V^2} \left( \int \mu\phi \right)^2 &= \frac{1}{2} \frac{N}{V^2} \left( \int \mu(\psi + \tilde{\phi}) \right)^2 \\
&= \frac{1}{2} \frac{N}{V^2} \left[ \left( \int \mu\psi \right)^2 + \left( \int \mu\tilde{\phi} \right)^2 + \left( \int \mu\psi \right) \left( \int \mu\tilde{\phi} \right) \right] \\
&= \frac{1}{2} \frac{N}{V^2} \left( \int \mu\psi \right)^2 + \frac{1}{2} N \tilde{\phi}^2 + \frac{N}{V} \tilde{\phi} \int \mu\psi
\end{aligned} \tag{A.3}$$

The last two terms follow since  $\int \mu\tilde{\phi} = V\tilde{\phi} = \int \mu\phi$ .

4.

$$\begin{aligned}
-\frac{N}{2V} \int \mu \phi^2 &= -\frac{1}{2} \frac{N}{V} \int \mu (\psi + \tilde{\phi})^2 \\
&= -\frac{1}{2} \frac{N}{V} \int \mu \psi^2 - \frac{1}{2} \frac{N}{V} \int \mu \tilde{\phi}^2 - \frac{N}{V} \tilde{\phi} \int \mu \psi \\
&= -\frac{1}{2} \frac{N}{V} \int \mu \psi^2 - \frac{1}{2} N \tilde{\phi}^2 - \frac{N}{V} \tilde{\phi} \int \mu \psi
\end{aligned} \tag{A.4}$$

5.

$$\begin{aligned}
i \frac{N}{V} \int \mu \phi &= i \frac{N}{V} \int \mu (\psi + \tilde{\phi}) \\
&= i \frac{N}{V} \int \mu \psi + i N \tilde{\phi}
\end{aligned} \tag{A.5}$$

Putting all these terms together one finds that the action becomes:

$$\begin{aligned}
\mathcal{H}[\psi(\vec{x})] &= -\frac{1}{2} \int \psi(\vec{x}) \left( -\nabla^2 + \frac{N}{V} \mu(\vec{x}) \right) \psi(\vec{x}) d\vec{x} + \frac{iN}{V} \int \mu(\vec{x}) \psi(\vec{x}) d\vec{x} - iz_m \int \delta(\vec{x}) \psi(\vec{x}) d\vec{x} \\
&\quad + \frac{N}{2V^2} \left( \int \mu(\vec{x}) \psi(\vec{x}) \right)^2 - \frac{1}{2} \tilde{\phi}(\vec{x}) \left( \int \nabla^2 \psi(\vec{x}) d\vec{x} + i(z_m - N) \right)
\end{aligned}$$

## APPENDIX B

### Calculation of the Green's function for the $\ell = 0$ channel

In this appendix we give the explicit calculation of the Green's function for the  $l = 0$  channel. The Green's function is the solution to the following equation;

$$(-\nabla^2 + \kappa^2\mu)G(r, r') = \delta(r - r'), \quad (\text{B.1})$$

subject to the following boundary conditions:

$$G_-(a, r') = G_+(a, r') \quad (\text{B.2})$$

$$\left. \frac{dG_-(r, r')}{dr} \right|_{r=a} = \left. \frac{dG_+(r, r')}{dr} \right|_{r=a} \quad (\text{B.3})$$

$$\left. \frac{dG_+(r, r')}{dr} \right|_{r=R} = 0 \quad (\text{B.4})$$

Where the  $+$  in  $G_{\pm}$  denotes the Green's Function for the regions  $r > a$  and the  $-$  sign the Green's function for the region  $r < a$ . When  $r \neq r'$ , we have to solve the homogeneous equation

$$(-\nabla^2 + \kappa^2\mu)G(r, r') = 0. \quad (\text{B.5})$$

The solution for the  $l = 0$  channel is

$$g(r, r') = \begin{cases} \left( \frac{A(r')}{r} + B(r') \right) \theta(a - r) + \left( C(r') \frac{e^{-\kappa r}}{r} + D(r') \frac{e^{\kappa r}}{r} \right) \theta(r - a) & \text{for } r < r' \\ \left( \frac{A'(r')}{r} + B'(r') \right) \theta(a - r) + \left( C'(r') \frac{e^{-\kappa r}}{r} + D'(r') \frac{e^{\kappa r}}{r} \right) \theta(r - a) & \text{for } r > r' \end{cases}$$

In the above equation  $\theta(x)$  denotes the usual Heaviside function. In order to ensure that the Green's function is regular at the origin, we set  $A(r') = 0$ . If we now apply the boundary conditions.

If we apply the boundary conditions to the solution for  $r < r'$  we have the following relations: Continuity of the Green's function at  $r = a$  gives

$$B(r') = C(r') \frac{e^{-\kappa a}}{a} + D(r') \frac{e^{-\kappa a}}{a} \quad (\text{B.6})$$

Continuity of the derivative gives

$$\begin{aligned} 0 &= -C(r')e^{-\kappa a}(\kappa a + 1) + D(r')e^{-\kappa a}(\kappa a - 1) \\ C(r') &= \frac{e^{2\kappa a}(\kappa a - 1)}{(\kappa a + 1)}D(r') \end{aligned} \quad (\text{B.7})$$

From these two equations we obtain

$$\begin{aligned} D(r') &= \frac{e^{-\kappa a}(\kappa a + 1)}{2\kappa}B(r') \\ &= \beta B(r') \end{aligned} \quad (\text{B.8})$$

and

$$\begin{aligned} C(r') &= \frac{e^{\kappa a}(\kappa a - 1)}{2\kappa}B(r') \\ &= \alpha B(r') \end{aligned} \quad (\text{B.9})$$

For the solution for  $r > r'$  we have the following: Continuity of the Green's function at  $r = a$  gives

$$\frac{A'(r')}{a} + B'(r') = C'(r')\frac{e^{-\kappa a}}{a} + D'(r')\frac{e^{-\kappa a}}{a} \quad (\text{B.10})$$

Continuity of the derivative gives

$$A'(r') = C'(r')e^{-\kappa a}(\kappa a + 1) - D'(r')e^{-\kappa a}(\kappa a - 1) \quad (\text{B.11})$$

The derivative at  $r = R$  set to zero gives

$$C'(r') = \frac{e^{2\kappa R}(\kappa R - 1)}{(\kappa R + 1)}D'(r') \quad (\text{B.12})$$

From these three equations one eventually obtains

$$C'(r) = \left( \frac{e^{2\kappa R}(\kappa R - 1)}{e^{\kappa a}(\kappa R + 1) - e^{2\kappa R}e^{-\kappa a}(\kappa R - 1)} \right) \frac{B'(r)}{\kappa} \quad (\text{B.13})$$

$$= \tilde{\alpha}B'(r'), \quad (\text{B.14})$$

$$\begin{aligned}
D'(r') &= \left( \frac{\kappa R + 1}{e^{\kappa a}(\kappa R + 1) - e^{2\kappa R}e^{-\kappa a}(\kappa R - 1)} \right) \frac{B'(r)}{\kappa} \\
&= \tilde{\beta} B'(r')
\end{aligned} \tag{B.15}$$

and

$$\begin{aligned}
A'(r') &= \left( \frac{e^{2\kappa R}e^{-\kappa a}(\kappa R - 1)(\kappa a + 1) - e^{\kappa a}(\kappa a - 1)(\kappa R + 1)}{e^{\kappa a}(\kappa R + 1) - e^{2\kappa R}e^{-\kappa a}(\kappa R - 1)} \right) \frac{B'(r)}{\kappa} \\
&= \tilde{\gamma} B'(r').
\end{aligned} \tag{B.16}$$

Therefore we have

$$g(r, r') = \begin{cases} B(r') [\theta(a - r) + (\alpha \frac{e^{-\kappa r}}{r} + \beta \frac{e^{\kappa r}}{r}) \theta(r - a)] & \text{for } r < r' \\ B'(r') [(\frac{\tilde{\gamma}}{r} + 1) \theta(a - r) + (\tilde{\alpha} \frac{e^{-\kappa r}}{r} + \tilde{\beta} \frac{e^{\kappa r}}{r}) \theta(r - a)] & \text{for } r > r' \end{cases}$$

Now to factorise, we write

$$g(r, r') = \tilde{B} \left[ \theta(a - r_{<}) + (\alpha \frac{e^{-\kappa r_{<}}}{r_{<}} + \beta \frac{e^{\kappa r_{<}}}{r_{<}}) \theta(r_{<} - a) \right] \left[ (\frac{\tilde{\gamma}}{r_{>}} + 1) \theta(a - r_{>}) + (\tilde{\alpha} \frac{e^{-\kappa r_{>}}}{r_{>}} + \tilde{\beta} \frac{e^{\kappa r_{>}}}{r_{>}}) \theta(r_{>} - a) \right], \tag{B.17}$$

where  $r_{<}$  ( $r_{>}$ ) denote the smaller (larger) one of  $r$  and  $r'$ . We now determine the normalisation constant  $\tilde{B}$  from the discontinuity of the derivative of  $g$  at  $r = r'$ . That is we use the relation

$$\left\{ \frac{d}{dr} [r g(r, r')] \right\}_{r'+\epsilon} - \left\{ \frac{d}{dr} [r g(r, r')] \right\}_{r'-\epsilon} = -\frac{1}{r'}. \tag{B.18}$$

To simplify the notation we denote the Green's function above by the following shorthand notation

$$g = \tilde{B} g_{<g>} \tag{B.19}$$

We first consider  $r < a$ . For  $r = r' + \epsilon$  we have  $r = r_{>}$  and  $r' = r_{<}$ . Thus we take the derivative with respect to  $r_{>}$ .

$$\begin{aligned}
\frac{d}{dr}[rg(r, r')] &= \tilde{B}g_{<} \frac{d}{dr}[rg_{>}] \\
&= \tilde{B}g_{<} \frac{d}{dr} \left[ r \frac{r\tilde{\gamma}}{r} + r \right] \\
&= \tilde{B}g_{<}
\end{aligned} \tag{B.20}$$

By the same procedure we obtain for  $r = r' - \epsilon$

$$\frac{d}{dr}[rg(r, r')] = \tilde{B}g_{>} \tag{B.21}$$

Therefore we have

$$\tilde{B}g_{<} - \tilde{B}g_{>} = -\frac{1}{r'}, \tag{B.22}$$

which eventually leads to

$$\tilde{B} = \frac{1}{\tilde{\gamma}} \tag{B.23}$$

If we follow exactly the same procedure as outlined above, we find that for  $r > a$

$$\tilde{B} = -\frac{1}{2\kappa(\alpha\tilde{\beta} - \tilde{\alpha}\beta)}. \tag{B.24}$$

For our calculation to be consistent, these two values for the normalisation constant have to be the same in both regions. If we substitute the expressions for  $\tilde{\gamma}$ ,  $\alpha$ ,  $\beta$ ,  $\tilde{\alpha}$  and  $\tilde{\beta}$  into the r.h.s. of eqs.(B.23) and (B.24), we see they are the same, and therefore our calculation is consistent.

## APPENDIX C

### The Partition Function for the case of added salt

In this Appendix we briefly show how the results for the partition function discussed in Chapter 2 change with the addition of salt. We will only highlight the results since the derivation is exactly the same as that presented in the main text.

The dimensionless Hamiltonian of this system is

$$\beta H = \frac{\ell_B}{2} \int d\vec{x}_1 \int d\vec{x}_2 \rho(\vec{x}_1) \frac{1}{|\vec{x}_1 - \vec{x}_2|} \rho(\vec{x}_2), \quad (\text{C.1})$$

where  $\beta = \frac{1}{k_B T}$  and  $\ell_B = \frac{e^2}{4\pi\epsilon k_B T}$  is the Bjerrum length. The charge density is given by

$$\rho(\vec{x}) = \rho_m(\vec{x}) - \rho_c(\vec{x}) + \rho_+(\vec{x}) - \rho_-(\vec{x}) \quad (\text{C.2})$$

$$= z_m \delta(\vec{x}) - z_c \sum_{i=1}^{N_c} \delta(\vec{x} - \vec{x}_i) + z_+ \sum_{j=1}^{N_+} \delta(\vec{x} - \vec{x}_j) - z_- \sum_{k=1}^{N_-} \delta(\vec{x} - \vec{x}_k), \quad (\text{C.3})$$

with  $\rho_m(\vec{x})$  the macromolecule charge density,  $\rho_c(\vec{x})$  the counterion charge density,  $\rho_+(\vec{x})$  the charge density of positive salt ions and  $\rho_-(\vec{x})$  the negative salt ion density. The  $z_i$  are the valencies of the different species of charged particles.

The canonical partition function is

$$\begin{aligned} Z &= \left[ \prod_{i=1}^{N_c} \int \frac{d\vec{x}_i}{V} \mu(\vec{x}_i) \right] \left[ \prod_{j=1}^{N_+} \int \frac{d\vec{x}_j}{V} \mu(\vec{x}_j) \right] \left[ \prod_{k=1}^{N_-} \int \frac{d\vec{x}_k}{V} \mu(\vec{x}_k) \right] e^{-\beta H} \\ &= \left[ \prod_{i=1}^{N_c} \int \frac{d\vec{x}_i}{V} \mu(\vec{x}_i) \right] \left[ \prod_{j=1}^{N_+} \int \frac{d\vec{x}_j}{V} \mu(\vec{x}_j) \right] \left[ \prod_{k=1}^{N_-} \int \frac{d\vec{x}_k}{V} \mu(\vec{x}_k) \right] e^{-\frac{\ell_B}{2} \int d\vec{x}_1 \int d\vec{x}_2 \rho(\vec{x}_1) \frac{1}{|\vec{x}_1 - \vec{x}_2|} \rho(\vec{x}_2)}. \end{aligned}$$

After performing the Hubbard-Stratonovich transformation to go over to the field theoretic formulation, the partition function becomes

$$\begin{aligned} Z &= \int [\mathcal{D}\phi] \left[ \prod_{i=1}^{N_c} \int \frac{d\vec{x}_i}{V} \mu(\vec{x}_i) \right] \left[ \prod_{j=1}^{N_+} \int \frac{d\vec{x}_j}{V} \mu(\vec{x}_j) \right] \left[ \prod_{k=1}^{N_-} \int \frac{d\vec{x}_k}{V} \mu(\vec{x}_k) \right] e^{-\frac{1}{8\pi\ell_B} \int d\vec{x} \phi(\vec{x}) (-\nabla^2) \phi(\vec{x})} \\ &\quad \times e^{i \int d\vec{x} (\rho_m(\vec{x}) - \rho_c(\vec{x}) + \rho_+(\vec{x}) - \rho_-(\vec{x})) \phi(\vec{x})}. \end{aligned}$$

Inserting the expression for the ion charge densities from eq.(C.3) into the functional

integral and explicitly performing the integration over the smaller ion coordinates, the following expression is obtained

$$\begin{aligned}
Z &= \int [\mathcal{D}\phi] e^{-\frac{1}{8\pi\ell_B} \int d\vec{x} \phi(\vec{x})(-\nabla^2)\phi(\vec{x}) + i \int d\vec{x} \rho_m(\vec{x})\phi(\vec{x})} \left( \frac{1}{V} \int d\vec{x} \mu(\vec{x}) e^{-iz_c\phi(\vec{x})} \right)^{N_c} \\
&\times \left( \frac{1}{V} \int d\vec{x} \mu(\vec{x}) e^{-iz_+\phi(\vec{x})} \right)^{N_+} \left( \frac{1}{V} \int d\vec{x} \mu(\vec{x}) e^{-iz_-\phi(\vec{x})} \right)^{N_-} \\
&= \int [\mathcal{D}\phi] e^{-\frac{1}{8\pi\ell_B} \int d\vec{x} \phi(\vec{x})(-\nabla^2)\phi(\vec{x}) + i \int d\vec{x} \rho_m(\vec{x})\phi(\vec{x}) + N_c \ln \left( \frac{1}{V} \int d\vec{x} \mu(\vec{x}) e^{-iz_c\phi(\vec{x})} \right)} \\
&\times e^{N_+ \ln \left( \frac{1}{V} \int d\vec{x} \mu(\vec{x}) e^{-iz_+\phi(\vec{x})} \right) + N_- \ln \left( \frac{1}{V} \int d\vec{x} \mu(\vec{x}) e^{-iz_-\phi(\vec{x})} \right)}. \tag{C.4}
\end{aligned}$$

We see that the only difference to the case without salt is the appearance of two additional factors, both of the same form as for the case with counterions only. As in the main text, we again approximate the logarithmic terms in the exponential and after employing precisely the same strategy for each of the three terms as presented in the text, one obtains the following linearised action for the functional integral

$$\begin{aligned}
\mathcal{H}[\phi] &= -\frac{1}{8\pi\ell_B} \int d\vec{x} \phi(\vec{x})(-\nabla^2)\phi(\vec{x}) - i \int d\vec{x} \rho_m(\vec{x})\phi(\vec{x}) \\
&= i(n_c z_c + n_+ z_+ + n_- z_-) \int d\vec{x} \mu(\vec{x})\phi(\vec{x}) - \frac{1}{2}(n_c z_c^2 + n_+ z_+^2 + n_- z_-^2) \int d\vec{x} \mu(\vec{x})\phi^2(\vec{x}) \\
&+ \frac{1}{2}(N_c z_c^2 + N_+ z_+^2 + N_- z_-^2) \left( \frac{1}{V} \int d\vec{x} \mu(\vec{x})\phi(\vec{x}) \right)^2.
\end{aligned}$$

where  $n_i = \frac{N_i}{V}$  (with  $i = c, +, -$ ) are the concentrations of the different species of ions in the solution. After following all of the remaining steps as explained in the text, one finds the partition function

$$Z = \int [\mathcal{D}\psi] e^{-\frac{1}{8\pi\ell_B} \int d\vec{x} \psi(\vec{x}) [-\nabla^2 + \kappa^2 \mu(\vec{x})] \psi(\vec{x}) + i \int d\vec{x} \rho_m(\vec{x})\psi(\vec{x})}, \tag{C.5}$$

with a redefined inverse screening length  $\kappa^2 = 4\pi\ell_B(n_c z_c^2 + n_+ z_+^2 + n_- z_-^2)$ . We see that the resultant field theory is of exactly the same form as for the case without salt, except with a different screening length. All of the qualitative features of the analysis presented for the case without salt therefore carry over to the case with additional salt, only with a modified screening length.



## BIBLIOGRAPHY

- [1] John C. Crocker and David G. Grier. When like charges attract: The effects of geometrical confinement on long-range colloidal interactions. *Phys. Rev. Lett.*, 77(9):1897–1900, Aug 1996.
- [2] D. G. Grier and Y. Han. Anomalous interactions in confined charge-stabilized colloid. *Journal of Physics: Condensed Matter*, 16:S4145–S4157, 2004.
- [3] Grace Martinelli Kepler and Seth Fraden. Attractive potential between confined colloids at low ionic strength. *Phys. Rev. Lett.*, 73(2):356–359, Jul 1994.
- [4] John C. Butler, Thomas Angelini, Jay X. Tang, and Gerard C. L. Wong. Ion multivalence and like-charge polyelectrolyte attraction. *Phys. Rev. Lett.*, 91(2):028301, Jul 2003.
- [5] Yan Levin. Electrostatic correlations: from plasma to biology. *Reports on Progress in Physics*, 65(11):1577–1632, 2002.
- [6] Luc Belloni. Ionic condensation and charge renormalization in colloidal suspensions. *Colloids and Surfaces A: Physicochemical and Engineering Aspects*, 140(1-3):227 – 243, 1998.
- [7] A R Denton. Charge renormalization, effective interactions, and thermodynamics of deionized colloidal suspensions. *Journal of Physics: Condensed Matter*, 20(49):494230, 2008.
- [8] S. Alexander, P. M. Chaikin, P. Grant, G. J. Morales, P. Pincus, and D. Hone. Charge renormalization, osmotic pressure, and bulk modulus of colloidal crystals: Theory. *The Journal of Chemical Physics*, 80(11):5776–5781, 1984.
- [9] Ali Naji and Roland R. Netz. Scaling and universality in the counterion-condensation transition at charged cylinders. *Physical Review E*, 73:056105, 2006.
- [10] R.R. Netz and H. Orland. Variational charge renormalization in charged systems. *European Physical Journal E*, 11:301, 2003.
- [11] I. Borukhov, D. Andelman, and H. Orland. Adsorption of large ions from an electrolyte solution: a modified poisson-boltzmann equation. *Electrochimica Acta*, 46(2-3):221 – 229, 2000.
- [12] Itamar Borukhov. Charge renormalization of cylinders and spheres: Ion size effects. *Journal of Polymer Science Part B: Polymer Physics*, 42:3598–3615, 2004.
- [13] Lyderic Bocquet, Emmanuel Trizac, and Miguel Aubouy. Effective charge saturation in colloidal suspensions. *The Journal of Chemical Physics*, 117(17):8138–8152, 2002.
- [14] Emmanuel Trizac and Gabriel Téllez. Onsager-manning-oozawa condensation phenomenon and the effect of salt. *Phys. Rev. Lett.*, 96(3):038302, Jan 2006.
- [15] Ali Naji, Svetlana Jungblut, Andr G. Moreira, and Roland R. Netz. Electrostatic interactions in strongly coupled soft matter. *Physica A: Statistical Mechanics and its Applications*, 352(1):131 – 170, 2005.
- [16] Markus Deserno, Christian Holm, and Sylvio May. Fraction of condensed counterions around a charged rod: Comparison of poisson-boltzmann theory and computer simulations. *Macromolecules*, 33(1):199–206, 2000.
- [17] A. Naji and R.R. Netz. Attraction of like-charged macroions in the strong-coupling limit. *The European Physical Journal E: Soft Matter and Biological Physics*, 13:43–59, 2004. 10.1140/epje/e2004-00039-x.
- [18] D. Andelman. Chapter 12 electrostatic properties of membranes: The poisson-boltzmann theory. In R. Lipowsky and E. Sackmann, editors, *Structure and Dynamics of Membranes - Generic and Specific Interactions*, volume 1, Part 2 of *Handbook of Biological Physics*, pages 603 – 642. North-Holland, 1995.

- [19] Markus Deserno and Christian Holm. Cell model and poisson-boltzmann theory: A brief introduction. In P. Kkicheff C. Holm and R Podgornik, editors, *Electrostatic Effects in Soft Matter and Biophysics*, volume 46 of *NATO Science Series II*,. Kluwer Academic Publishers, 2001.
- [20] Emmanuel Trizac and Jean-Pierre Hansen. Wigner-seitz model of charged lamellar colloidal dispersions. *Phys. Rev. E*, 56(3):3137–3149, Sep 1997.
- [21] R. R. Netz and H. Orland. Field theory for charged fluids and colloids. *EPL (Europhysics Letters)*, 45(6):726–732, 1999.
- [22] Jean-Pierre Hansen and Hartmut Löwen. Effective interactions between electric double-layers. *Annu. Rev. Phys. Chem.*, 51:209–242, 2000.
- [23] Marcia C. Barbosa, Markus Deserno, Christian Holm, and René Messina. Screening of spherical colloids beyond mean field: A local density functional approach. *Phys. Rev. E*, 69(5):051401, May 2004.
- [24] Luc Belloni and Olivier Spalla. Attraction of electrostatic origin between colloids. *Journal of Chemical Physics*, 107(2):465, 1997.
- [25] Luc Belloni. Colloid-counterion mixtures: an advanced integral equation. *Journal of Physics: Condensed Matter*, 14(40):9323–9337, 2002.
- [26] Roland Kjellander. Distribution function theory of electrolytes and electrical double layers charge renormalisation and dressed ion theory. In P. Kkicheff C. Holm and R Podgornik, editors, *Electrostatic Effects in Soft Matter and Biophysics*, volume 46 of *NATO Science Series II*,, pages 317 – 364. Kluwer Academic Publishers, 2001.
- [27] Niels Grønbech-Jensen, Robert J. Mashl, Robijn F. Bruinsma, and William M. Gelbart. Counterion-induced attraction between rigid polyelectrolytes. *Phys. Rev. Lett.*, 78(12):2477–2480, Mar 1997.
- [28] Per Linse and Vladimir Lobaskin. Electrostatic attraction and phase separation in solutions of like-charged colloidal particles. *Phys. Rev. Lett.*, 83(20):4208–4211, Nov 1999.
- [29] V. Lobaskin, A. Lyubartsev, and P. Linse. Effective macroion-macroion potentials in asymmetric electrolytes. *Phys. Rev. E*, 63:020401–1 – 020401–4, 2001.
- [30] E. Allahyarov, I. D’Amico, and H. Löwen. Attraction between like-charged macroions by coulomb depletion. *Phys. Rev. Lett.*, 81(6):1334–1337, Aug 1998.
- [31] Robert D. Groot. Ion condensation on solid particles: Theory and simulations. *The Journal of Chemical Physics*, 95(12):9191–9203, 1991.
- [32] A.G. Moreira and R.R. Netz. Simulations of counterions at charged plates. *The European Physical Journal E: Soft Matter and Biological Physics*, 8:33–58, 2002. 10.1140/epje/i2001-10091-9.
- [33] R Podgornik. An analytic treatment of the first-order correction to the poisson-boltzmann interaction free energy in the case of counterion-only coulomb fluid. *Journal of Physics A: Mathematical and General*, 23(3):275–284, 1990.
- [34] R.R. Netz and H. Orland. Beyond poisson-boltzmann: Fluctuation effects and correlation functions. *The European Physical Journal E*, 1(2/3):203–214, 2000.
- [35] A. W. C. Lau, D. B. Lukatsky, P. Pincus, and S. A. Safran. Charge fluctuations and counterion condensation. *Phys. Rev. E*, 65(5):051502, Apr 2002.
- [36] A. W. C. Lau and P. Pincus. Counterion condensation and fluctuation-induced attraction. *Phys. Rev. E*, 66:041501–1 – 041501–14, 2002.

- [37] B.-Y. Ha and A. J. Liu. Counterion-mediated attraction between two like-charged rods. *Phys. Rev. Lett.*, 79:1289–1292, 1997.
- [38] B.-Y. Ha and A. J. Liu. Effect of non-pairwise-additive interactions on bundles of rodlike polyelectrolytes. *Phys. Rev. Lett.*, 81:1011–1014, 1998.
- [39] B.-Y. Ha and A. J. Liu. Counterion-mediated, non-pairwise-additive attractions in bundles of like-charged rod. *Phys. Rev. E.*, 60:803–813, 1999.
- [40] M. Kardar and R. Golestanian. The 'friction' of vacuum, and other fluctuation-induced forces. *Rev. Mod. Phys.*, 71:1233, 1999.
- [41] R.R. Netz. Electrostatics of counter-ions at and between planar charged walls: From poisson-boltzmann to the strong-coupling theory. *The European Physical Journal E: Soft Matter and Biological Physics*, 5:557–574, 2001. 10.1007/s101890170039.
- [42] André G. Moreira and Roland R. Netz. Binding of similarly charged plates with counterions only. *Phys. Rev. Lett.*, 87(7):078301, Jul 2001.
- [43] G.S. Manning. *J. Chem. Phys.*, 51:924, 1969.
- [44] J. C. Neu. Wall-mediated forces between like-charged bodies in an electrolyte. *Phys. Rev. Lett.*, 82:1072–1074, 1999.
- [45] Leonard I. Schiff. *Quantum Mechanics*. McGraw-Hill Kogakusha, third edition, 1968.
- [46] Jörg Baumgartl, Jose Luis Arauz-Lara, and Clemens Bechinger. Like-charge attraction in confinement: myth or truth? *Soft matter*, 2:631–635, 2006.
- [47] Niels Grnbech-Jensen, Keith M. Beardmore, and Philip Pincus. Interactions between charged spheres in divalent counterion solution. *Physica A: Statistical and Theoretical Physics*, 261(1-2):74 – 81, 1998.
- [48] Gerald V Dunne and Klaus Kirsten. Functional determinants for radial operators. *Journal of Physics A: Mathematical and General*, 39(38):11915–11928, 2006.
- [49] Klaus Kirsten and Alan J. McKane. Functional determinants by contour integration methods. *Annals of Physics*, 308(2):502 – 527, 2003.
- [50] Klaus Kirsten and Alan J McKane. Functional determinants for general sturm-liouville problems. *Journal of Physics A: Mathematical and General*, 37(16):4649–4670, 2004.
- [51] John David Jackson. *Classical Electrodynamics*. Wiley, third edition, 1999.
- [52] René van Roij, Marjolein Dijkstra, and Jean-Pierre Hansen. Phase diagram of charge-stabilized colloidal suspensions: van der waals instability without attractive forces. *Phys. Rev. E*, 59(2):2010–2025, Feb 1999.
- [53] Klaus Kirsten. *Spectral Functions in Mathematics and Physics*. Chapman & Hall/CRC, 2002.
- [54] Klaus Kirsten and Paul Loya. Calculation of determinants using contour integrals. *American Journal of Physics*, 76:60, 2008.